

Scalar-Mediated Quantum Forces Between Macroscopic Bodies and Interferometry

Philippe Brax ^{a*} and Sylvain Fichet ^{b,c†}

^a *Institut de Physique Théorique, Université Paris-Saclay, CEA, CNRS,
F-91191 Gif/Yvette Cedex, France*

^b *ICTP South American Institute for Fundamental Research & IFT-UNESP,
R. Dr. Bento Teobaldo Ferraz 271, São Paulo, Brazil*

^c *Centro de Ciências Naturais e Humanas, Universidade Federal do ABC,
Santo Andre, 09210-580 SP, Brazil*

Abstract

We study the quantum force between classical objects mediated by massive scalar fields bilinearly coupled to matter. The existence of such fields is motivated by dark matter, dark energy, and by the possibility of a hidden sector beyond the Standard Model. We introduce the quantum work felt by an arbitrary (either rigid or deformable) classical body in the presence of the scalar and show that it is finite upon requiring conservation of matter. As an example, we explicitly show that the quantum pressure inside a Dirichlet sphere is finite — up to renormalizable divergences. With this method we compute the scalar-induced quantum force in simple planar geometries. In plane-point geometry we show how to compute the contribution of the quantum force to the phase shift observable in atom interferometers. We show that atom interferometry is likely to become a competitive search method for light particles bilinearly coupled to matter, provided that the interferometer arms have lengths below ~ 10 cm.

*phbrax@gmail.com

†sfichet@caltech.edu

Contents

1	Introduction	3
2	The Quantum Work	6
2.1	Action and Quantum Vacuum Energy	6
2.2	The Source and its Deformation	7
2.3	Quantum Work and Force	8
2.4	W_λ is Finite (Renormalizable Case)	10
3	Weak Coupling: Finiteness Properties and Thin Shell Limit	12
3.1	W_λ is Finite (EFT Case)	13
3.2	The Thin Shell Limit	14
3.3	The Dirichlet Limit	16
4	Scalar Quantum Forces between Rigid Bodies	17
4.1	Rigid Bodies	17
4.2	Vanishing of Tadpoles	18
4.3	The Scalar Casimir-Polder Limit	18
4.4	The Scalar Casimir Limit	19
5	The Dirichlet Sphere	19
5.1	Is the quantum pressure on the sphere finite in QFT?	19
5.2	Review and Discussion	20
5.3	The Quantum Work on the Dirichlet Sphere	21
6	Planar Geometry	22
6.1	Force Between two Plates	22
6.2	Force Between a Plate and a Point Source	25
7	Bounding Quantum Forces with Atom Interferometry	28
7.1	The setting	28
7.2	Computing the Phase Shift	29
7.3	Limits	30
7.4	Sensitivity to New Particles	31
8	Conclusion	33
A	Derivation of the Plate-Point Casimir-Polder Potential	34
B	On Divergences from the Heat Kernel Expansion	36
C	The Loop Divergence from Momentum Space	37

1 Introduction

The exchange of virtual particles induces macroscopic forces between bodies. Beyond the tree level, such forces are relativistic and quantum in essence, they are properly described in the framework of quantum field theory (QFT). Here we refer to such forces simply as “quantum forces”. Even though the seminal works on Casimir forces are from the nineteen forties [1, 2], the topic of quantum forces is still very much active (see *e.g.* [3–9] for recent papers and reviews). In the case of electromagnetic interactions, refined calculations take into account medium properties such as electromagnetic permittivities as well as effects from finite temperature, see [10] for a comprehensive review. In the present paper we work in the simple framework of scalar-mediated quantum forces at zero temperature, with the key assumption that the scalar couples bilinearly to the sources.² In this scalar setting, we use a simple variational method to derive quantum forces between bodies of various shapes and positions.

The scalar case is of prime relevance for cosmology [15, 16] and deriving quantum forces mediated by massive scalars could lead to new laboratory tests of important cosmological models, from scalar dark matter to dark energy. In this paper, we argue that atom interferometry [17] could be such a promising technique. Our primary motivation comes from the pervasiveness of scalar fields bilinearly coupled to matter in cosmology [16] and in extensions of the Standard Model of particle physics [18]. For instance, the dark matter in our Universe can be modelled as a scalar particle with Z_2 symmetry, which couples thus bilinearly to matter. A wealth of dark energy models and related modified gravity models [19] also involve a light scalar field. For these, when the classical force induced by the linear coupling to sources is screened (see *e.g.* [20–22]), the quantum force arising from the bilinear coupling to sources can become dominant [23], hence motivating our study. Finally, irrespective of observational motivations, the existence of a sector hidden beyond the Standard Model and featuring a light scalar with a Z_2 symmetry (*e.g.* a pseudo-Nambu Goldstone boson of a symmetry of the hidden sector) is a logical possibility that requires investigation. There is thus, in short, a cornucopia of reasons to study scalar fields bilinearly coupled to matter.

A secondary motivation is that some of the technical and conceptual results that we present — such as the proof of finiteness of the quantum work — are best exposed with a scalar field. We use an approach based on the variation of the quantum vacuum energy which is similar in spirit to the one found in the seminal work by Schwinger [24]. The developments presented here can be taken as a streamlined presentation of this variational method based in the context of scalar QFT.

The vacuum energy of QFT features divergences which are treated via standard renormalization methods, *e.g.* using dimensional regularization and introducing local counterterms [25], which maps these divergences onto the RG flow of the Lagrangian parameters. The fact that such divergences do not affect the quantum force can be shown in complete generality at one-loop using *e.g.* the heat kernel expansion [10]. Apart from these

²See *e.g.* [11–14] for a selection of related works involving scalar quantum forces.

well-behaved divergences, other “spurious” divergences which are non-removable by renormalization can appear in certain Casimir calculations. This happens for example for a calculation of the pressure in the Dirichlet sphere [26] (see detailed discussion in Sec. 5), and even for a version of the calculation of the pressure between plates (see detailed discussion in Sec. 6.1). While such spurious divergences might be easily identified and removed in an ad hoc way, in this work we will show that they are systematically removed by the requirement of conservation of matter in the sources. Matter conservation has so far not been taken into account in calculations of quantum forces, to the best of our knowledge. At the conceptual level it is the new ingredient of our calculations.

Hopefully our presentation will be useful to cosmologists who would like to see their models tested in the laboratory. In particular we transparently explain in terms of Feynman diagrams how the screening of the scalar inside the sources gives rise to two distinct regimes for the quantum force. This situation is similar to the Casimir and Casimir-Polder forces arising in electromagnetism. The common nature and unified description of these electromagnetic quantum forces has been long known, see *e.g.* Refs. [24, 27]. Here we will give a formula for the quantum force in the massive scalar case and relate the “scalar Casimir” and “scalar Casimir-Polder” forces.³ The use of this general formula is mandatory for computing certain observables such as phase shifts in interferometry.

Finally, another purpose of this work is to lay out the foundations for more phenomenological studies, for which the effect of the quantum force from a particle beyond the Standard Model needs to be predicted in realistic experiments. As such, we will present a calculation of the phase shift induced by a quantum force and measurable in atom interferometers. We will then study to which extent atom interferometry is a competitive method to search for light dark particles.

Technical Review

The present study bears some technical similarities with other works from the Casimir literature. Here we briefly list a few of these references. Our definition of the quantum work involves the variation of the quantum vacuum energy with respect to a deformation of the source. A similar approach relying on energy variation has been used in [24], expressed in the language of Schwinger’s source theory. The source we consider has finite density, and the Dirichlet limit is obtained by sending the density to infinity. A similar framework was considered in [12, 33, 34] (the conservation equation is not exploited in these references). In our formalism we consider arbitrary deformations of an arbitrary body. A somewhat similar approach was taken in [24] in the case of deformation of a dielectric fluid. We sometimes use regularisation by point-splitting, in the context of Casimir calculations this method has for example been used in [3]. Finally, under certain conditions including that the bodies are incompressible, finiteness of the quantum work at one-loop can be shown using the heat kernel formalism. This is reviewed and discussed in App. B.

Comparison to [35] : After pre-publication we became aware of the recent article [35] whose scope and results have partial overlap with the present study — upon appropriate

³See *e.g.* [28–32] for Casimir-Polder-like forces in the context of particle physics.

matching of terms and concepts. Both works introduce the concept of variable/effective mass. The *principle of virtual work* whose proof for arbitrary geometry in a specific model is presented in [35] is fully compatible with the general formula of the *quantum work* presented here. The translation of the key quantities between the model of [35] and the present work is $\phi|_{[35]} \equiv \Phi$, $\frac{\lambda_1}{4}\sigma^2\phi^2|_{[35]} \equiv \mathcal{B}_m J$. An important difference of scope is that in [35] the deformation flow of the body is rigid, which implies that no discussion of matter conservation is needed. In contrast, the compressible deformation flow and its relation to matter conservation are a key aspect of our study. Finally, the formula for the quantum work resulting from the rigid deformation of an interface is obtained in [35] in terms of a surface integral of the stress tensor. This result turns out to precisely match the one we obtain in our Eq. (3.21) upon setting the variation of density to zero, even though the intermediate steps of the derivations are rather different. This is a nontrivial verification of the consistency of both works.

Outline

The paper is arranged as follows. Section 2 presents the framework for scalar quantum forces, giving a formula for the quantum work valid at the non-perturbative level for arbitrary deformable sources. Section 3 specializes to the weak coupling case (which includes the case of effective field theories). The quantum work in the limiting case of thin-shell geometries is further evaluated. Section 4 specializes to two rigid bodies, showing that the Casimir and Casimir-Polder forces for massive scalar fields are asymptotically recovered as limits of our unifying formula for quantum forces. The Casimir pressure on the Dirichlet sphere is revisited and shown to be finite in section 5. The generalized Casimir forces for finite density objects and a finite vacuum mass for the scalar field in plane-plane and point-plane geometry are respectively computed in sections 6. In section 7 we then calculate the phase shift in atom interferometers. In App. A we compare a computation of the Casimir-Polder interaction from a scattering amplitude and our derivation, showing explicitly that they coincide. In App. B we review a proof of the finiteness of the quantum work at the one-loop level using the heat kernel expansion following the steps of [10], which contributes to motivating our approach. App. C contains details on a loop calculation in momentum space .

Definitions and Conventions

We assume $d + 1$ -dimensional Minkowski spacetime \mathcal{M}_{d+1} with mostly-minus signature $(+, -, \dots, -)$. The $d + 1$ Cartesian coordinates are denoted by x_μ , spatial coordinates are denoted by $x_i \equiv \mathbf{x}$. We will be considering a source $J(\mathbf{x})$ with arbitrary shape and dimension. The support of the source is described by the indicator function $\mathbf{1}_J(\mathbf{x})$ or equivalently using a continuous support function $l(\mathbf{x})$ which is positive where J is supported and negative where it is not, with $\mathbf{1}_J(x) \equiv \Theta(l(\mathbf{x}))$ where Θ is the Heaviside distribution. The boundary of the source is denoted by $\partial J = \{\mathbf{x} \in \mathcal{M}_{d+1} | l(\mathbf{x}) = 0\}$. Integration over the support of the source J is denoted $\int_J d^d \mathbf{x}$. Integration over the support of the boundary ∂J is denoted $\int_{\partial J} d\sigma(\mathbf{x})$. Although our main focus is ultimately the $d = 3$ case, we keep d general when possible and specialize to $d = 3$ in specific settings.

2 The Quantum Work

In this section we compute the quantum work felt by a source bilinearly coupled to a quantum field under an arbitrary deformation of the source. We focus on a scalar field Φ for simplicity — generalization to spinning fields is identical although more technical. The bodies subject to the Casimir forces are assumed to be classical and static. The set of bodies is collectively represented in the partition function by a static source term $J(\mathbf{x})$. More precisely, the $J(\mathbf{x})$ distribution corresponds to the vacuum expectation of the density operator $\hat{n}(\mathbf{x})$ in the presence of matter, $J(\mathbf{x}) = \langle \Omega | \hat{n}(\mathbf{x}) | \Omega \rangle$.

2.1 Action and Quantum Vacuum Energy

We consider the fundamental Lagrangian

$$\mathcal{L}[\Phi] = \frac{1}{2}(\partial_M \Phi)^2 - \frac{1}{2}m^2\Phi^2 + \dots \quad (2.1)$$

The ellipses include possible interactions of Φ , which do not need to be specified. The interacting theory for Φ can either be renormalizable — with either weak or strong coupling, or may also be an effective field theory (EFT) involving a series of operators of arbitrary dimensions. In this latter case the theory is weakly coupled below the EFT cutoff scale on distances larger than $\Delta x \sim \frac{1}{\Lambda}$. The scale Λ is the energy cut-off of the theory.

We consider the partition function in Minkowski spacetime⁴

$$Z[J] = \int \mathcal{D}\Phi e^{i(S[\Phi] - \int d^{d+1}x \mathcal{B}[\Phi]J(\mathbf{x}))} \quad (2.2)$$

where $\mathcal{B}[\Phi]$ is a bilinear operator in Φ . This operator can encode an arbitrary number of field derivatives. We distinguish two cases. If the bilinear operator has no derivative, then the scalar theory can be renormalizable. In this case we write the operator as

$$\mathcal{B}_m[\Phi] = \frac{1}{2\Lambda}\Phi^2 \quad (2.3)$$

If the bilinear operator has derivatives, then the scalar theory is an EFT and in general contains a whole series of higher dimensional operators. In this case, including an arbitrary number of such terms, we can write the operator as

$$\mathcal{B}_{\text{EFT}}[\Phi] = \sum_{n>1,i} \frac{c_{n,i}}{2\Lambda^{2n+1}} \Phi \mathcal{O}_{n,i} \Phi \quad (2.4)$$

where $\mathcal{O}_{n,i}$ is a scalar derivative operator with $2n$ derivatives which act either to the left or to the right,⁵

$$\mathcal{O}_{n,i} = (\overleftarrow{\partial}^2)^p \overleftarrow{\partial}_{\mu_1} \dots \overleftarrow{\partial}_{\mu_a} (\overrightarrow{\partial}^2)^{n-p-a} \overrightarrow{\partial}_{\mu_1} \dots \overrightarrow{\partial}_{\mu_a} \quad (2.5)$$

⁴We call the generating functional $Z[J]$ the partition function in analogy to the Euclidean case.

⁵When writing the bilinear interaction in the form Eq. (2.4), consistently with the source term defined in (2.2), we take into account that any derivative acting on J has been removed using integration by part, producing derivatives that act on the fields. With this constraint, the most general structure is the one given in Eq. (2.5).

The $c_{n,i}$ coefficients are dimensionless.

Let us comment further about some aspects of EFT. Here we distinguished between the \mathcal{B}_m and \mathcal{B}_{EFT} operators, essentially because our subsequent analysis of finiteness of the quantum work slightly differs between both cases. In general, a given EFT can feature both the \mathcal{B}_m and \mathcal{B}_{EFT} terms. In such case the \mathcal{B}_m contribution would tend to dominate, unless it is suppressed by a symmetry (*e.g.* a shift symmetry). Still in the EFT framework, we may also notice that non-derivative higher order operators involving powers of Φ and J are in general present. While the higher order operators which are bilinear in Φ could be simply accounted in the generic source J , the broader view is that the EFT validity domain prevents these operators from becoming important, *i.e.* schematically $\partial/\Lambda \ll 1$. Finally we emphasize that our subsequent analyses involving UV divergences can be done at the level of the EFT, without having to specify the underlying completion, see *e.g.* [36, 37] for more details on divergences and renormalization in EFT.

Since the source is static, the partition function takes the form

$$Z[J] = e^{-iE[J]T} \quad (2.6)$$

where $E[J]$ is referred to as the *quantum vacuum energy* and T is an arbitrary time interval specified in evaluating the time integrals. This time scale will drop from the subsequent calculations.⁶ In general, we can set J as an abstract quantity that can be used to generate the correlators of the theory. In our case, since the source couples to \mathcal{B} (see Eq. (2.2)), taking functional derivatives of $E[J]$ in J generates the connected correlators of the composite operator \mathcal{B} , *i.e.* $\langle \mathcal{B}(x_1)\mathcal{B}(x_2)\dots \rangle$. In this work, we consider that J represents a physical distribution of matter, *i.e.* $J(\mathbf{x})$ is taken to be the expectation value of the density operator $\hat{n}(\mathbf{x})$ in the presence of matter, $J(\mathbf{x}) = \langle \Omega | \hat{n}(\mathbf{x}) | \Omega \rangle$. For concreteness, one can for instance think of a nonrelativistic fermion density, appearing for example via $\bar{\psi}\psi = n(\mathbf{x})$ or $\bar{\psi}\gamma_\mu\psi = \delta_{\mu 0}n(\mathbf{x})$ in the relativistic formulation.⁷

2.2 The Source and its Deformation

The source is parametrized by

$$J(\mathbf{x}) = n(\mathbf{x})\mathbf{1}_J(\mathbf{x}) \quad (2.7)$$

and corresponds to a particle number distribution of mass dimension d . The support of this distribution is encoded in $\mathbf{1}_J(\mathbf{x}) = \Theta(l(\mathbf{x}))$ where the continuous function $l(\mathbf{x})$ is positive where J is supported and negative where it is not. The number density $n(\mathbf{x})$ is in general an arbitrary distribution over the support. The integral $N_J = \int d\mu_i J(\mu_i)$ amounts to the total particle number of the source.

⁶In Minkowski space we have in general $Z = \langle 0 | e^{-i\mathcal{H}T} | 0 \rangle$, with \mathcal{H} the Hamiltonian of the system. This is why the eigenvalue $E[J]$ is identified as the vacuum energy. We also mention that upon Wick rotation to Euclidean space, $E[J]$ corresponds to the free energy of the system.

⁷Higher monomials contributions such as $\frac{(\bar{\psi}\psi)^2}{\Lambda^3}$ are neglected in this example. We mention that in the presence of screening, *i.e.* in the Dirichlet or Casimir regime defined in next sections, the validity of the EFT tends to be improved because the coupling to the source tends to be suppressed. Validity of the EFT in the presence of screening has been discussed in [23].

We then introduce a deformation of the source. We assume that matter is deformable *i.e.* both the support and the number density can vary under the deformation. We will see that such a generalization from rigid to deformable matter is necessary in order to ensure that the calculation is well-defined and that no infinities show up.

The infinitesimal deformation of the source is parametrized by a scalar parameter λ . Under our assumptions the source depends on this deformation parameter as $J_\lambda(\mathbf{x}) = n_\lambda(\mathbf{x})\Theta[l_\lambda(\mathbf{x})]$. The deformed source takes the form $J_{\lambda+d\lambda}(\mathbf{x}) = n_{\lambda+d\lambda}(\mathbf{x})\Theta[l_{\lambda+d\lambda}(\mathbf{x})]$. The deformation of the support of the source is parametrized by

$$l_{\lambda+d\lambda}(\mathbf{x}) = l_\lambda(\mathbf{x} - \mathbf{L}(\mathbf{x})d\lambda) \quad (2.8)$$

where the \mathbf{L} vector is the deformation flow. Defining $\frac{\partial}{\partial \lambda} \equiv \partial_\lambda$ the variation of the source under the λ deformation is then given by $\partial_\lambda J_\lambda(\mathbf{x}) = \partial_\lambda n_\lambda \Theta[l_\lambda(\mathbf{x})] - n_\lambda \mathbf{L} \cdot \boldsymbol{\partial} l_\lambda \delta[l_\lambda(\mathbf{x})]$. An arbitrary deformation of a generic source is pictured in Fig. 1.

We assume that $J(\mathbf{x})$ is made out of classical matter and is not a completely abstract distribution. As the source is made of classical matter, then its *local number density must be conserved*. Any deformation of the source must be therefore subject to the conservation of the number density. The local conservation equation under the deformation parametrized by λ is

$$\partial_\lambda n_\lambda + \boldsymbol{\partial} \cdot (n_\lambda \mathbf{L}) = 0. \quad (2.9)$$

It implies the integral form

$$\partial_\lambda \int_{J_\lambda} d^d \mathbf{x} n_\lambda(\mathbf{x}) = \int d^d \mathbf{x} \partial_\lambda J_\lambda(\mathbf{x}) = 0 \quad (2.10)$$

where the second integral is over all space.

In the special case where the density n is constant in λ and x , Eq. (2.9) reduces to the condition of an incompressible deformation flow, $\boldsymbol{\partial} \cdot \mathbf{L} = 0$. In this case the source describes incompressible matter (e.g. a fluid). If $\boldsymbol{\partial} \cdot \mathbf{L} = 0$ and \mathbf{L} is piecewise constant in x , then the source describes *rigid* matter. Section. 4 specializes to such rigid sources.

2.3 Quantum Work and Force

We now study how the quantum system evolves upon a general, infinitesimal deformation of the source, $\lambda \rightarrow \lambda + d\lambda$. To proceed we introduce the quantum work under a variation in λ ,

$$W_\lambda = -\partial_\lambda E[J_\lambda]. \quad (2.11)$$

In the particular case of a rigid body and if the deformation field can be factored out, then a quantum force can be defined as

$$W_\lambda = \mathbf{L} \cdot \mathbf{F}. \quad (2.12)$$

This defines the quantum force between the objects. Such a simplification is however generally not possible, the most fundamental quantity to consider is the quantum work. Our definition of quantum work is closely related to variational approaches such as the

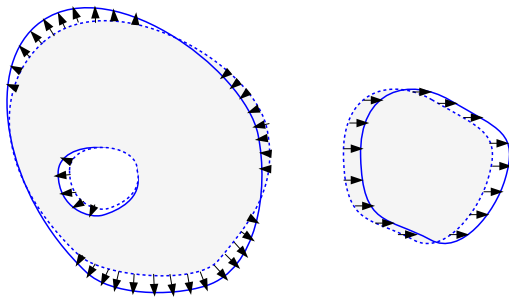


Figure 1. An arbitrary infinitesimal deformation of a generic source. The dotted and plain contours respectively correspond to the boundary of J_λ and $J_{\lambda+d\lambda}$. The arrows denote the deformation flow \mathbf{L} .

principle of virtual work applied to quantum physics, see *e.g.* [24] and [38, 39] for related recent studies.

The quantum vacuum energy $E[J]$ is a formally divergent quantity. However, if one varies it with respect to a physical parameter, the resulting variation is a physical observable and thus should be finite.⁸ Hence even though W_λ encodes all the quantum effects felt by the source(s), the only divergences remaining in this quantity are those with a physical meaning, *i.e.* the ones which must be treated in the framework of renormalization. One origin for such divergences is the field interactions, another can be the curvature of spacetime, as pointed out in [40] in AdS. Even for a free theory in flat space, there can be renormalization of surface tension terms, as pointed out in [41]. We refer to such divergences as “physical” ones — these are the familiar divergences from QFT, that only appear for specific integer values of spacetime dimension. One of our goals in the following is to show that there are no other divergences than the physical ones in the QFT calculation of the quantum force.

Using the definition of Eqs. (2.2), (2.6), the quantum work is given by

$$W_\lambda = - \int d^d \mathbf{x} \langle \mathcal{B} \rangle_{J_\lambda} (x, x) \partial_\lambda J_\lambda(\mathbf{x}) \quad (2.13)$$

where $\langle \mathcal{B} \rangle_{J_\lambda}$ is the time-ordered quantum average of \mathcal{B} in the presence of the source J_λ . Here and throughout we use the shortcut notation $W_{J_\lambda} = W_\lambda$, $\langle \mathcal{B} \rangle_{J_\lambda} = \langle \mathcal{B} \rangle_\lambda$. While all quantities depend on λ , the λ dependence is relevant only under the ∂_λ variation and is often dropped elsewhere. The two-point function in presence of the source at coinciding points will be sometimes denoted by $\langle \mathcal{B} \rangle_J$ in the rest of the paper.

Using the general form of the bilinear coupling, \mathcal{B} is expressed in terms of the two point function of Φ in the presence of J , $\langle T\Phi(x)\Phi(y) \rangle_J$, evaluated at coinciding points. We assume that the classical value of Φ is zero.⁹ Hence the disconnected part of the two-point

⁸Throughout this work, the physical parameter is typically a geometric variable such as the distance between two bodies.

⁹This can be the consequence of a Z_2 symmetry, enforcing that Φ only appears bilinearly in the action such that $\langle \Phi \rangle = 0$. In the presence of nonzero $\langle \Phi \rangle$, the possible Z_2 symmetry is broken, implying that at

function vanishes and the two-point function reduces to $\langle T\Phi(x)\Phi(y)\rangle_J = \Delta_J(x, y)$, where $\Delta_J(x, y)$ is the Feynman propagator in the presence of the source J . The quantum average of \mathcal{B} is then expressed in terms of the Feynmann propagator Δ_J as

$$\langle \mathcal{B}_m \rangle_J = \frac{1}{2\Lambda} \Delta_J(x_1, x_2) \quad (2.14)$$

$$\langle \mathcal{B}_{\text{EFT}} \rangle_J = \sum_{n>1, i} \frac{c_{n,i}}{2\Lambda^{2n+1}} \mathcal{O}_{n,i} \Delta_J(x_1, x_2). \quad (2.15)$$

Here in the EFT case we introduce the shortcut $\langle T\Phi(x)\mathcal{O}_{n,i}\Phi(y)\rangle_J \equiv \mathcal{O}_{n,i}\Delta_J(x, y)$ where the $\mathcal{O}_{n,i}$ operator as defined in Eq. (2.5) has derivatives acting to the left and to the right. The general formula for the quantum work presented in Eq. (2.13) is valid at the non-perturbative level.

2.4 W_λ is Finite (Renormalizable Case)

The quantity $\langle \mathcal{B} \rangle_J(x, x)$ is formally divergent since it contains the propagator at coinciding points. It is thus not obvious why the quantum work W_λ should be finite. Throughout this subsection, we regulate the divergence in $\langle \mathcal{B} \rangle_J$ by introducing a small splitting of the endpoints, $\langle \mathcal{B} \rangle_J(x, x) \equiv \langle \mathcal{B} \rangle_J(x, x_\epsilon)|_{\epsilon \rightarrow 0}$ where we defined $x_\epsilon = x + \epsilon$.¹⁰

We consider the renormalizable case *i.e.* the $\langle \mathcal{B} \rangle_m$ operator (the EFT case is addressed in section 3.1). We assume that, as a preliminary step, all the divergences which can be removed by the renormalization of the coupling constants of local operators have been performed, *e.g.* the fundamental mass m is the renormalized mass. We assume that $n(\mathbf{x})$ is *finite* for any \mathbf{x} over the support of J (the $n \rightarrow \infty$ limit is discussed in section 3.2). No assumption on the interactions of Φ is necessary thus Φ can be strongly coupled. Under these conditions the finiteness of the quantum work can be shown as follows.

In the $\epsilon \rightarrow 0$ limit, we can decompose the expectation value of \mathcal{B} as the sum of *i)* the ϵ -dependent, would-be divergent term, and *ii)* a finite term in which the ϵ dependence amounts to $O(\epsilon)$ corrections that can be neglected for $\epsilon \rightarrow 0$. This gives

$$\langle \mathcal{B} \rangle_J(x, x_\epsilon) = \langle \mathcal{B} \rangle_J^{\text{div}}(x, x_\epsilon) + \langle \mathcal{B} \rangle_J^{\text{fin}}(x, x) + O(\epsilon). \quad (2.16)$$

We then use the assumption that the number density is finite. It implies that the effective squared mass of Φ inside the source, $m^2 + \frac{n(\mathbf{x})}{\Lambda}$, is finite. We remind that m has been renormalized already. A divergence in the short distance behaviour of $\langle \mathcal{B} \rangle(x, x_\epsilon)$ can arise from a propagator going from x to x_ϵ . As the effective mass term amounts to a *relevant*

weak coupling the fluctuation of Φ over the $\langle \Phi \rangle$ background has a linear coupling to the source. As a result a classical force is also present in addition to the quantum force. This case does not need to be investigated in the present paper. This extra classical force appearing in the presence of $\langle \Phi \rangle \neq 0$ does not automatically dominate over the quantum force — instead, various regimes arise as a function of the geometry. These aspects have been partly investigated in [23].

¹⁰The analogous regularization in Fourier space is momentum cutoff, $p < \frac{1}{\epsilon}$. These regularizations admit a physical meaning. ϵ can be thought as the distance scale below which the description of the classical matter as a continuous distribution breaks down. In this view, the cutoff length ϵ has a physically meaningful value, and the statement of existence of a divergence turns into a statement on ϵ -dependence of the result.

operator with finite value, it is negligible in the short distance limit of the propagator, *i.e.* in the large momentum limit. As the source J appears in the propagator only via the effective mass term, we conclude that the divergent piece $\langle \mathcal{B} \rangle_J^{\text{div}}(x, x_\epsilon)$ is independent of J . Furthermore, in that short distance limit, the propagator must be Lorentz invariant, and we conclude that the divergent piece in Eq. (2.16) is independent of x ,

$$\langle \mathcal{B} \rangle_J^{\text{div}}(x, x_\epsilon)|_{\text{small } \epsilon} = \langle \mathcal{B} \rangle^{\text{div}}(x, x_\epsilon) = \langle \mathcal{B} \rangle^{\text{div}}(0, \epsilon) \equiv \langle \mathcal{B} \rangle_\epsilon^{\text{div}}. \quad (2.17)$$

We thus see that the divergent piece depends only on ϵ and diverges in the $\epsilon \rightarrow 0$ limit. Using the decomposition Eq. (2.16) and the definition of the quantum work, we obtain the decomposition

$$W_\lambda = W_\lambda^{\text{fin}} + W_\lambda^{\text{div}} \quad (2.18)$$

with

$$W_\lambda^{\text{fin,div}} = - \int d^d \mathbf{x} \langle \mathcal{B} \rangle_J^{\text{fin,div}}(x, x) \partial_\lambda J_\lambda(\mathbf{x}). \quad (2.19)$$

In the divergent piece, $\langle \mathcal{B} \rangle_\epsilon^{\text{div}}$ factors out of the integral because it is independent of x . This gives

$$W_\lambda^{\text{div}} = - \langle \mathcal{B} \rangle_\epsilon^{\text{div}} \int d^d \mathbf{x} \partial_\lambda J_\lambda(\mathbf{x}). \quad (2.20)$$

The remaining integral corresponds exactly to the variation of the total density of the source under the deformation, appearing in the integral form of the conservation equation Eq. (2.10). Thus if the equation of conservation Eq. (2.10) is satisfied, then Eq. (2.20) vanishes. We conclude that, upon conservation of matter in the source, for any deformation and finite n the quantum work is finite:

$$W_\lambda^{\text{div}} = 0. \quad (2.21)$$

This is true at the nonperturbative level. In the particular case of incompressible matter, Eq. (2.20) reduces to

$$W_\lambda^{\text{div}}|_{\text{incompressible}} = -n \langle \mathcal{B} \rangle^{\text{div}} \int_J d^d \mathbf{x} \boldsymbol{\partial} \cdot L(\mathbf{x}). \quad (2.22)$$

In that case we can say that, upon conservation of matter in the source, for any divergent-free deformation flow and finite n , the quantum work is finite:

$$W_\lambda^{\text{div}}|_{\text{incompressible}} = 0 \quad (2.23)$$

The finiteness of the quantum work will be exemplified in the upcoming sections.

Finally we comment on the finite part of the quantum work. The finite part can be put in the useful alternative form by evaluating the integrand, using the divergence theorem and using the conservation equation,

$$W_\lambda^{\text{fin}} = - \int d^d \mathbf{x} n_\lambda(\mathbf{x}) \mathbf{L} \cdot \boldsymbol{\partial} [\langle \mathcal{B} \rangle_\lambda(x, x)]. \quad (2.24)$$

This is another way to verify that any constant piece in $\langle \mathcal{B} \rangle(x, x)$ does not contribute to the quantum work as it appears under a gradient in the integrand.

3 Weak Coupling: Finiteness Properties and Thin Shell Limit

At weak coupling the Φ field has an equation of motion (EOM) that we can use to evaluate the quantum work. We introduce the bilinear operator \mathcal{B}'' , defined by

$$\mathcal{B} = \frac{1}{2}\Phi(x)\mathcal{B}''\Phi(x). \quad (3.1)$$

This is the operator that appears in the EOM. For example, when applied to \mathcal{B}_m this is $\mathcal{B}_m'' = \frac{1}{\Lambda}$. In the EFT case, \mathcal{B}'' is the differential operator appearing in Eq. (2.4),

$$\mathcal{B}_{\text{EFT}}'' = \sum_{n>1,i} \frac{c_{n,i}}{\Lambda^{2n+1}} \mathcal{O}_{n,i}. \quad (3.2)$$

The left and right derivatives in $\mathcal{O}_{n,i}$ act on the propagators attached respectively to the left and right of the vertex.

At leading order in the perturbative expansion, the $\Delta_J(x, x')$ propagator satisfies the equation of motion

$$\mathcal{D}_x \Delta_J(x, x') + \mathcal{B}'' J(\mathbf{x}) \Delta_J(x, x') = -i\delta^{d+1}(x - x') \quad (3.3)$$

where $\mathcal{D} = \square + m^2$ is the wave operator and \square is the scalar d'Alembertian. The solution to Eq. (3.3) is a Born series that describes the bare propagator Δ_0 (*i.e.* $\Delta_J|_{J \rightarrow 0}$) dressed by insertions of $\mathcal{B}'' J$. For convenience we define the insertion

$$\Sigma(x, y) = -i\mathcal{B}'' J(\mathbf{x})\delta^{d+1}(x - y) \quad (3.4)$$

and we use the inner product $f \star g = \int d^{d+1}u f(u)g(u)$. With these definitions the dressed propagator is given by

$$\Delta_J(x, x') = \sum_{q=0}^{\infty} \Delta_0 [\star \Sigma \star \Delta_0]^q(x, x') \quad (3.5)$$

$$= \Delta_0(x, x') - \int d^{d+1}u \Delta_0(x, u) i\mathcal{B}'' J(\mathbf{u}) \Delta_0(u, x') + \dots \quad (3.6)$$

Putting this result back into Eq. (2.13) provides the leading, one-loop contribution to the quantum work,¹¹

$$W_\lambda^{1\text{-loop}} = -\frac{1}{2\Lambda} \int d^d \mathbf{x} \mathcal{B}'' \sum_{q=0}^{\infty} \Delta_0 [\star \Sigma \star \Delta_0]^q(x, x) \partial_\lambda J(\mathbf{x}) \quad (3.7)$$

This is valid for both \mathcal{B}_m and \mathcal{B}_{EFT} insertions. In terms of Feynman diagrams Eq. (3.7) is simply a loop with an arbitrary number of insertions of $\mathcal{B}'' J$ and one insertion of $\partial_\lambda J$. A term of the series is represented (without the ∂_λ variation) in Fig. 2, where each insertion is represented by a black dot.

¹¹Another, conceptually similar way to derive this formula is via the heat kernel formalism, see *e.g.* [39, 41]

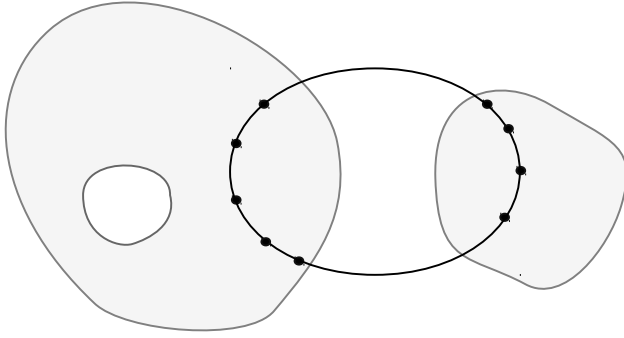


Figure 2. A sample one-loop diagram in the presence of an arbitrary source. Black dots represent insertions of $-i\mathcal{B}''J(\mathbf{x})$. Each black dot is integrated over the support of the source. Under an infinitesimal deformation of the source ($\lambda \rightarrow \lambda + d\lambda$), the corresponding variation (*i.e.* ∂_λ) of this diagram contributes to the one-loop quantum work Eq. (3.7).

In the EFT case, the validity domain of the EFT implies that higher derivatives terms in \mathcal{B}_{EFT} must remain small. Still, in the series of Eq. (3.7), the effect of lower derivative terms may become important in some regime. When the effect of these derivatives is important, it may happen that convergences issues in Eq. (3.7) appear, that need careful consideration taking into account EFT validity. A related example is discussed in details in [42]. In the following, we will show the finiteness of every term in $W_\lambda^{1\text{-loop}}$ and simply assume that the overall series is convergent.

3.1 W_λ is Finite (EFT Case)

Our proof of Eq. (2.21) uses that the effective mass is a relevant operator that becomes negligible at short distances. In contrast, the insertions from \mathcal{B}^{EFT} correspond to irrelevant operators hence the same reasoning cannot apply — the operators become more important at short distance. The solution to this apparent puzzle is that the EFT in its domain of validity is necessarily weakly coupled, hence instead of using a non-perturbative argument one can use the series representation Eq. (3.7) to prove finiteness.

Let us verify finiteness term-by-term. We single out a term from Eq. (3.7) and introduce point-splitting, $\mathcal{B}''\Delta_0[\star\Sigma\star\Delta_0]^q(x, x_\epsilon)$, with $x_\epsilon = x + \epsilon$. Our goal is to show that the divergent piece in this quantity is independent of x . The term is

$$\mathcal{B}''\Delta_0[\star\Sigma\star\Delta_0]^q(x, x_\epsilon) = (-i)^q \left(\prod_{i=1}^q \int d^d\mu_i J(\mu_i) \int dt_i \right) \prod_{i=0}^q \mathcal{B}''\Delta_0(\mu_i, \mu_{i+1}) \Big|_{\mu_0=x, \mu_{q+1}=x_\epsilon} \quad (3.8)$$

It is understood that one of the block of derivatives in \mathcal{B}'' acts to the left and the other acts to the right.

The divergence in the diagram defined by Eq. (3.8) occurs when all the positions coincide. This is more easily verified in momentum space, in which case there is a single loop integral over the internal momentum flowing around the loop. The divergence is tied to the large momentum for all the propagators, which in position space corresponds to the limit

of coincident endpoints. We present the explicit momentum space calculation in App. C. The divergent piece of Eq. (3.8) is $(-i)^q c_J^q L_{q,\epsilon}^{\text{div}}$ where c_J is finite and $L_{q,\epsilon}^{\text{div}}$ is the divergent part. The key point is that $L_{q,\epsilon}^{\text{div}}$ is position-independent.

Putting this piece into the definition of the quantum work Eq. (3.7) gives the divergent piece of the quantum work,

$$W_\lambda^{1-\text{loop,div}} = -\frac{1}{2\Lambda} \sum_{q=0}^{\infty} (-ic_J)^q L_{q,\epsilon}^{\text{div}} \int d^d \mathbf{x} \partial_\lambda J. \quad (3.9)$$

The remaining integral corresponds exactly to the variation of the total density of the source under the deformation, appearing in the integral form of the conservation equation Eq. (2.10). Thus if the equation of conservation Eq. (2.10) is satisfied, then Eq. (3.9) vanishes.

It follows that, upon conservation of matter in the source, for any deformation and finite n the quantum work is finite:

$$W_\lambda^{1-\text{loop,div}} = 0. \quad (3.10)$$

The incompressible version of this finiteness property trivially follows, like for Eq. (2.23).

3.2 The Thin Shell Limit

So far we have considered a generic source as an arbitrary volume in d -dimensional space. Here we investigate a subset of sources for which the support is a thin shell approaching a codimension-one hypersurface.

We denote the source by $J_\eta = n(x) \mathbf{1}_{\mathcal{S}_\eta, \lambda}(x)$ where η parametrizes the small width of the shell. For $\eta \rightarrow 0$ the support of the shell tends to a hypersurface denoted by \mathcal{S} . To avoid any ambiguity we always keep η small but nonzero in the following calculations. The volume element can be split as

$$\int_{\mathcal{S}_\eta} d^d \mathbf{x} \stackrel{\text{small } \eta}{=} \int_{\mathcal{S}} d\sigma(\mathbf{x}) \int_{\text{width}} dx_\perp \quad (3.11)$$

where the x_\perp coordinate parametrizes the direction normal to \mathcal{S} . The boundary of \mathcal{S}_η can also be decomposed as

$$\partial \mathcal{S}_{\eta \rightarrow 0} = \mathcal{S}_{\text{in}} \cup \mathcal{S}_{\text{out}} \quad (3.12)$$

where $\mathcal{S}_{\text{in, out}}$ are the two hypersurfaces bounding the volume enclosed by \mathcal{S}_η in the limit $\eta \rightarrow 0$. The propagator in the presence of the thin shell is denoted by $\Delta_{\mathcal{S}}(x, x')$. The density can be chosen to scale with η such that it remains finite for $\eta \rightarrow 0$. This happens if the density scales as $\eta n = \text{cst}$. In the following, the deformation of the source is kept arbitrary. All quantities depend on the deformation parameter λ . We will drop the λ index when appropriate.

We evaluate the quantum work for this specific class of sources, taking η small but finite. For simplicity we consider the coupling to the source induced via the \mathcal{B}_m operator. Our evaluation involves various manipulations of the EOMs and of the divergence theorem.

We emphasize that we do *not* use the conservation equation. That way we can explicitly demonstrate later on, at the level of applications, that the conservation equation is required to obtain finiteness of the quantum work. For clarity we split the calculation in various steps.

Step 1: Starting from the general expression of the quantum work Eq. (2.13), we evaluate the $\partial_\lambda J_\lambda$ variation. We use $\frac{\partial \mathbf{l}}{\|\partial \mathbf{l}\|} = \mathbf{n}_{\text{in}}$ with \mathbf{n}_{in} the inward-pointing normal vector, then use the divergence theorem $\int_{\partial \mathcal{S}} d\sigma(\mathbf{x}) \mathbf{n}_{\text{out}} \cdot \mathbf{f}(\mathbf{x}) = \int_{\mathcal{S}} d^d \mathbf{x} \partial(\mathbf{f}(\mathbf{x}))$ with $\mathbf{n}_{\text{out}} = -\mathbf{n}_{\text{in}}$. We obtain

$$W_{\mathcal{S}_\eta, \lambda} = -\frac{1}{2\Lambda} \int_{\mathcal{S}_\eta} d^d \mathbf{x} \Delta_{\mathcal{S}}(\mathbf{x}, \mathbf{x}) \partial_\lambda n_\lambda(x) - \frac{1}{2\Lambda} \int_{\mathcal{S}_\eta} d^d \mathbf{x} \partial[\mathbf{L} n_\lambda(x) \Delta_{\mathcal{S}}(x, x)]. \quad (3.13)$$

Step 2: (Using the equations of motion) We will further simplify the second term of Eq.(3.13) by observing that it can be related to discontinuities determined from the equation of motion. In order to proceed we introduce the notation for derivatives acting on either the first or second argument of the propagator, $\partial_1 \Delta(x, x') \equiv \partial_x \Delta(x, x')$, $\partial_2 \Delta(x, x') \equiv \partial_{x'} \Delta(x, x')$. The coincident-point propagator is regularized via point-splitting using $x_\epsilon = x + \epsilon$ where the shifted point is taken to belong to \mathcal{S} when $x \in \mathcal{S}$.

In the thin shell limit, the second term in Eq. (3.13) takes the form

$$-\frac{1}{2\Lambda} \eta \int_{\mathcal{S}} d\sigma(\mathbf{x}) (\partial_1[\mathbf{L}(x) n(x) \Delta_{\mathcal{S}}(x, x_\epsilon)] + \mathbf{L}(x) n(x) \partial_2[\Delta_{\mathcal{S}}(x, x_\epsilon)]) (1 + O(\eta)) \quad (3.14)$$

We used the volume element Eq. (3.11) and that the integrand is continuous over \mathcal{S}_η . In the first term of Eq. (3.14) the vector \mathbf{L} is kept inside the derivative for further convenience.

The EOM is

$$\mathcal{D}_x \Delta_{\mathcal{S}}(x, x') + \frac{1}{\Lambda} J_\eta(\mathbf{x}) \Delta_{\mathcal{S}}(x, x') = -i\delta^{d+1}(x - x') \quad (3.15)$$

where $\mathcal{D}_x = \square_x + m^2$. Below the δ^{d+1} is always zero due to point splitting. Each of the terms in Eq. (3.14) can be expressed using an appropriate derivative of the EOM, with the remaining endpoint set to an appropriate value.

The first term in Eq. (3.14) is obtained by multiplying the EOM with $\mathbf{L}(\mathbf{x})$ then applying ∂_x . We then integrate across the normal coordinate and set the remaining endpoint of the propagator x' to coincide with x in the transverse coordinates. This gives the identity

$$-\frac{\eta}{\Lambda} \partial_1[\mathbf{L} n \Delta_{\mathcal{S}}(x, x_\epsilon)] (1 + O(\eta)) \stackrel{\text{small } \eta}{=} \left[\int_{\text{width}} dx_\perp \partial_x [\mathbf{L}(\mathbf{x}) \square_x \Delta_{\mathcal{S}}(x, x')] \right]_{x' \rightarrow x_\epsilon} \quad (3.16)$$

The fundamental mass contributes as $O(\eta)$, it is thus neglected. After integrating over the transverse coordinates (*i.e.* applying $\int_{\mathcal{S}} d\sigma(\mathbf{x})$), the l.h.s of Eq. (3.16) coincides with the first term of Eq. (3.14).

The second term in Eq. (3.14) is obtained by applying $\partial_{x'}$ to the EOM then contracting with $\mathbf{L}(\mathbf{x}')$. The subsequent steps are the same as above and the result is

$$-\frac{\eta}{\Lambda} \mathbf{L} n \partial_2[\Delta_{\mathcal{S}}(x, x_\epsilon)] (1 + O(\eta)) \stackrel{\text{small } \eta}{=} \left[\int_{\text{width}} dx_\perp \mathbf{L}(\mathbf{x}') \partial_{x'} [\square_x \Delta_{\mathcal{S}}(x, x')] \right]_{x' \rightarrow x_\epsilon}. \quad (3.17)$$

Using the identities (3.16) and (3.17) in Eq. (3.14) one can eliminate the presence of the density in favor of d'Alembertians.

Step 3: Finally we use the divergence theorem on the right hand side of both Eqs. (3.16) and (3.17). In Eq.(3.17) the divergence theorem turns the \square_x into $\mathbf{n} \cdot \partial$.¹² Replacing these results in Eq. (3.13) we obtain the final form for the quantum work on a thin shell,

$$W_\lambda^S = -\frac{1}{2} \int_{\mathcal{S}_{\text{in}} \cup \mathcal{S}_{\text{out}}} d\sigma(\mathbf{x}) \left(n_i L_j \partial_1^i \partial_2^j \Delta_S(x, x_\epsilon) + \mathbf{n} \cdot \mathbf{L} \square_1 \Delta_S(x, x_\epsilon) \right) - \frac{1}{2\Lambda} \int_{\mathcal{S}_\eta} d^d \mathbf{x} \Delta_S(x, x_\epsilon) \partial_\lambda n_\lambda(\mathbf{x}) + O(\eta) \quad (3.18)$$

The volume term in the second line encodes the variation of the number density of the source under the deformation. Notice that we have not used the conservation equation yet in deriving Eq. (3.18). The conservation equation must ensure that the quantum work is finite, along the line of (2.21). This will be exemplified in Sec. 5.

3.3 The Dirichlet Limit

We have so far assumed that $\eta n \equiv n_S$ is finite. n_S can be understood as the number density on the hypersurface \mathcal{S} . In this subsection we take the limit $n_S \rightarrow \infty$. In this limit we obtain that the propagator *vanishes* anywhere inside \mathcal{S}_η , including on the boundaries $\mathcal{S}_{\text{in}}, \mathcal{S}_{\text{out}}$, *i.e.* we have $\Delta_S(x, x') = 0$ for any x' or $x \in \mathcal{S}$. On the other hand the derivatives normal to the boundary do not vanish on the boundary, *i.e.* $\partial_1^\perp \Delta_S(x, x')|_{x \in \mathcal{S}_{\text{in}, \text{out}}} \neq 0$.¹³ In summary, the limit $n_S \rightarrow \infty$ amounts to a *Dirichlet boundary condition* for the propagator.

We now apply this Dirichlet limit to the quantum work Eq. (3.18). The second surface term in the first line of Eq. (3.18) vanishes in the Dirichlet limit since the second endpoint belongs to the boundary and has no derivative acting on it. In contrast the first surface term involves derivatives on both endpoints and thus does not vanish in the Dirichlet limit. This term further simplifies: the first derivatives of $\Delta(x, x')$ across \mathcal{S} are discontinuous only in the normal coordinate, while they are continuous in the other directions, therefore $n_i L_j \partial_1^i \partial_2^j \Delta_S(x, x_\epsilon) = L_\perp \partial_1^\perp \partial_2^\perp \Delta_S(x, x_\epsilon)$. We see that only the normal component of the deformation flow $L_\perp = \mathbf{n} \cdot \mathbf{L}$ contributes in the Dirichlet limit.

We can then make contact with the scalar stress-energy tensor $T^{\mu\nu} = -\partial^\mu \phi \partial^\nu \phi + \frac{1}{2} \eta^{\mu\nu} (\partial_\rho \phi \partial^\rho \phi - m^2 \phi^2)$. Namely, when considering the normal component $T^{\perp\perp}$, we recognize that the difference of the time-ordered expectation value $\langle T^{\perp\perp} \rangle$ between \mathcal{S}_{out} and \mathcal{S}_{in} is

$$\left[\langle T^{\perp\perp} \rangle \right]_{\mathcal{S}_{\text{in}}}^{\mathcal{S}_{\text{out}}} = \frac{1}{2} \left[\langle \partial^\perp \phi \partial^\perp \phi \rangle \right]_{\mathcal{S}_{\text{in}}}^{\mathcal{S}_{\text{out}}} = \frac{1}{2} \left[\partial_1^\perp \partial_2^\perp \Delta_S(x, x) \right]_{\mathcal{S}_{\text{in}}}^{\mathcal{S}_{\text{out}}} \quad (3.20)$$

¹²Notice that x' is set to x_ϵ only outside of the integral. Hence the x' dependence of the integrand is irrelevant when applying the divergence theorem.

¹³These properties are shown at the level of the EOM using field continuity. We integrate the EOM on any domain crossing \mathcal{S}_η and use the divergence theorem. This makes appear the well-known "jump" in the normal derivatives

$$\partial_1^\perp \Delta_S(x, x')|_{x \in \mathcal{S}_{\text{out}}} - \partial_1^\perp \Delta_S(x, x')|_{x \in \mathcal{S}_{\text{in}}} = \frac{n_S}{\Lambda} \Delta_S(x, x')|_{x \in \mathcal{S}} \times (1 + O(\eta)). \quad (3.19)$$

The propagator is continuous everywhere, hence on the rhs is it enough to simply write $x \in \mathcal{S}$ without further detail. Due to the requirement of continuity of the propagator, the discontinuity of derivatives must remain finite. As a result, taking the limit $n_S \rightarrow \infty$ implies that $\Delta_S(x, x')|_{x \in \mathcal{S}} \rightarrow 0$ for any x' .

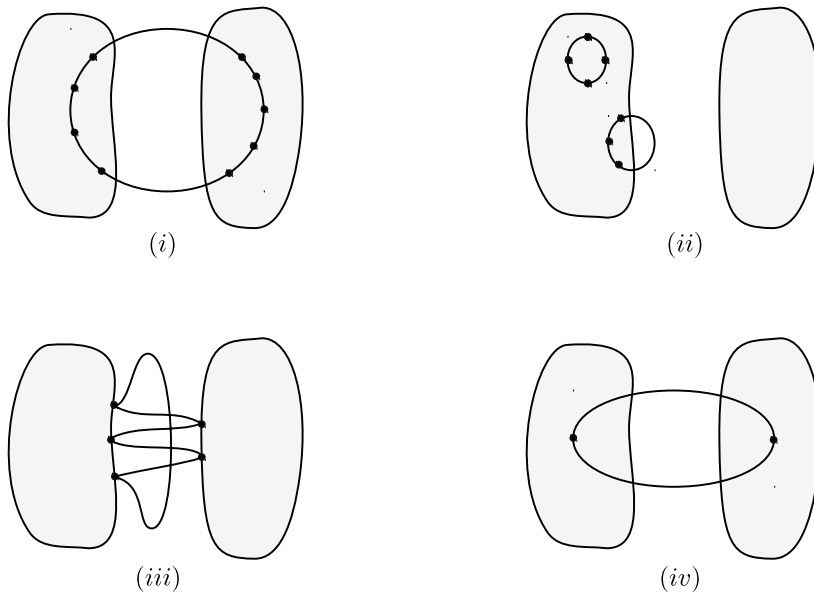


Figure 3. Sample Feynman diagrams for a scalar field in the presence of two extended sources. (i): A generic one-loop contribution. (ii): “Tadpole” loops vanishing under ∂_λ . (iii): Casimir limit (Strong coupling to sources) (iv): Casimir-Polder limit (Weak coupling to sources)

Notice that there is a contribution from the normal derivatives inside the isotropic $\eta_{\mu\nu}$ term. The derivatives in the transverse directions do not contribute due to continuity. It follows that the quantum work on a thin shell in the Dirichlet limit can be expressed using the stress-energy tensor as

$$W_\lambda^S = - \int_{\mathcal{S}_{\text{in}} \cup \mathcal{S}_{\text{out}}} d\sigma(\mathbf{x}) L_\perp \langle \Omega | T^{\perp\perp} | \Omega \rangle - \frac{1}{2\Lambda} \int_{\mathcal{S}_\eta} d^d \mathbf{x} \Delta_S(x, x_\epsilon) \partial_\lambda n_\lambda(\mathbf{x}) + O(\eta) \quad (3.21)$$

This is, of course, not a coincidence. This contribution to the quantum work reproduces exactly the difference of stress-energy tensors that is used to compute the Casimir forces or pressures on thin shells, see *e.g.* [26]. The second term, which is the new term arising in our calculation, must ensure that any spurious divergence arising from the first term cancels out upon requiring matter conservation of the source, as dictated by the finiteness property Eq. (2.21). We will exemplify this in the case of the Dirichlet sphere in Sec. 5.

4 Scalar Quantum Forces between Rigid Bodies

4.1 Rigid Bodies

In this section we choose a specific shape for the source and the deformation. The source is assumed to be the compound of two rigid bodies $J = J_1 + J_2$ with number densities $n_{1,2}$. We assume that the J_2 source moves rigidly with respect to J_1 . The deformation flow \mathbf{L} thus reduces to a constant vector over J_2 and vanishes elsewhere. In this particular case

the \mathbf{L} factors out in W_λ and we can talk about the quantum force $\mathbf{F}_{1\rightarrow 2}$ between J_1 and J_2 . Using Eq. (3.7) the general expression for the quantum work is expressed as

$$W_\lambda^{1\text{-loop}} = \mathbf{L} \cdot \mathbf{F}_{1\rightarrow 2} = -\frac{1}{2\Lambda} \int d^d \mathbf{x} \sum_{q=0}^{\infty} \Delta_0 [\star \Sigma \star \Delta_0]^q (x, x) \mathbf{L} \cdot \partial J_2(x) \quad (4.1)$$

where $\Sigma = -\frac{i}{\Lambda}(J_1 + J_2)\delta^{d+1}(x - y)$. We will then evaluate the general formula Eq. (4.1) in specific limits. An arbitrary term of the series is represented in Fig. 3*i*.

4.2 Vanishing of Tadpoles

In Eq. (4.1), each insertion of Σ contains both J_1 and J_2 . Let us focus on subterms involving only J_2 . Such terms amount to the generalization of “tadpole” diagrams for an extended source, here J_2 . Using integrations by parts and the fact that the propagators Δ_0 in empty spacetime are Lorentz invariant, *i.e.* are functions of $u - v$ only, one can check that any such tadpole term is equal to minus itself and thus vanishes. This makes sense since such terms do not involve the J_1 source at all and should not contribute to the force between the two sources. A tadpole diagram is represented in Fig. 3*ii*. These diagrams contain divergent contributions to the quantum work. Therefore the vanishing of the tadpole diagrams ensures that the perturbative finiteness Eq. (3.10) is satisfied.

4.3 The Scalar Casimir-Polder Limit

Let us assume that the values of $\frac{n_{1,2}}{\Lambda}$ are small enough such that the leading contributions come from the first terms in the series. The first term of the series has $q = 0$. This term amounts to a tadpole diagram, hence it vanishes as shown in Sec. 4.2. We thus turn to the $q = 1$ term. This term is

$$W_{q=1}^{1\text{-loop}} = \frac{i}{2\Lambda^2} \int d^d \mathbf{u} d^{d+1} v \Delta_0(u, v) J(v) \Delta_0(v, u) \mathbf{L} \cdot \partial J_2(u). \quad (4.2)$$

We then decompose $J(u) = J_1(u) + J_2(u)$. The $\int J_2 \Delta_0^2 \partial J_2$ piece is again a tadpole and thus vanishes as shown in Sec. 4.2 — using integration by parts, one can check that it is equal to minus itself. The remaining term is

$$W_{q=1}^{1\text{-loop}} = \frac{i}{2\Lambda^2} \int d^d \mathbf{u} d^{d+1} v \Delta_0(u, v) J_1(v) \Delta_0(v, u) \mathbf{L} \cdot \partial J_2(u). \quad (4.3)$$

Upon integrating by parts (or evaluating ∂J_2 and using the divergence theorem), we recognize the variation of a bubble diagram that corresponds precisely to the definition of the Casimir-Polder potential $V_{\text{CP}}(R)$ between two point sources. Namely,

$$W_{q=1}^{1\text{-loop}} = -n_1 n_2 \int d^d \mathbf{u} d^d \mathbf{v} \mathbf{L} \cdot \partial V_{\text{CP}}(u - v) \quad (4.4)$$

where we have defined the potential

$$V_{\text{CP}}(r) = -\frac{i}{2} \int dt (\Delta_0(0; r, t))^2 = -\frac{1}{32\pi^3 \Lambda^2} \frac{m}{r^2} K_1(2mr). \quad (4.5)$$

We can see the explicit dependence on the fundamental mass m in this result. Details of the explicit evaluation in the last step can be found in *e.g.* Ref. [32].

We can notice that Eq. (4.4) amounts to the integral over the $J_{1,2}$ supports of the quantum work between two point sources generated by the directional derivative of the potential W_{CP} , i.e. $W_{n=1}^{1-\text{loop}} = n_1 n_2 \int d^d \mathbf{u} d^d \mathbf{v} W_{\text{CP}}$ with $W_{\text{CP}} = -\mathbf{L} \cdot \partial V_{\text{CP}}$.

A diagram in the Casimir-Polder limit is shown in Fig. 3iv. In this limit the quantum loop penetrates the whole bodies.

4.4 The Scalar Casimir Limit

A different limit is obtained when the effective mass inside the sources, $m^2 + \frac{n_{1,2}(\mathbf{x})}{\Lambda}$, is large enough for the dressed propagator to be repelled from the sources. This occurs whenever $\mathcal{D}_x \Delta(x, x') \ll J(\mathbf{x}) \Delta_J(x, x')$ for any x, x' . In this Dirichlet limit, the EOM Eq. (3.3) gives then $J(\mathbf{x}) \Delta_J(x, x') \approx 0$, which enforces $\Delta_J(x, x') \approx 0$ for any x in the source and any x' in the whole space. The propagator vanishes on the boundary, $\Delta_J(x \in \partial J, x') \approx 0$, by continuity. Therefore the propagator has Dirichlet boundary conditions in this regime. We refer to this limit as the scalar Casimir limit since it reproduces a Dirichlet problem for which the quantum force is usually referred to as "Casimir" even when the underlying theory is not electrodynamics, e.g. here a massive scalar field theory.

A sample diagram from the Casimir limit is shown in Fig. 3iii. In this limit the quantum loop does not penetrate inside the bodies.

Summarizing, we have shown that our formula for the one-loop quantum work Eq.(4.1) interpolates between the scalar Casimir-Polder force and the scalar Casimir force. The two limits are realised in different physical regimes, which essentially depend on the competition between the magnitudes of the effective mass and of the d'Alembertian in the EOM. Qualitatively, we can say that for fixed fundamental parameters and densities, the Casimir-Polder limit emerges in the *short separation* regime while the Casimir limit emerges in the *large separation* regime.

5 The Dirichlet Sphere

In this section we consider the Casimir pressure on a spherical shell in the presence of a scalar field with Dirichlet boundary condition on the shell, *i.e.* a "Dirichlet sphere". This is a standard problem, that we wish here to revisit. An early calculation can be found in [43], and an expression describing the Casimir pressure on a $d - 1$ -sphere has been derived in [26], which will be our main reference.

5.1 Is the quantum pressure on the sphere finite in QFT?

The QFT prediction obtained in [26] features a "spurious" divergence. Here we discuss why such a divergence is not expected in light of the finiteness properties derived in Sec. 2. We have emphasised in Sec. 2 the role of matter conservation to obtain a finite quantum work. In the case of the sphere, the deformation flow describing the radial deformation of the sphere is not divergence-free, $\partial \cdot L_{\text{Sphere}} \neq 0$ for arbitrary spacetime dimension d except

$d = 1$. If the sphere density were to be assumed to be constant, then the matter of the sphere would *not* be conserved under the deformation and it would then follow that neither of the finiteness properties (2.21) and (2.23) would apply. Hence a divergent piece would show up in the expression of the quantum pressure as an artefact. This is exactly what we find below. We also show how this spurious divergence exactly cancels when matter conservation is used.

5.2 Review and Discussion

We first review the result from [26]. The radius of the sphere is denoted by a . The pressure on the sphere obtained in this reference can be put in the form

$$\frac{F_{S_{d-1},[26]}}{A_{d-1}} = \frac{F_{S_{d-1},[26]}^{\text{fin}}}{A_{d-1}} + \frac{F_{S_{d-1},[26]}^{\text{div}}}{A_{d-1}} \quad (5.1)$$

where

$$\begin{aligned} \frac{F_{S_{d-1},[26]}^{\text{fin}}}{A_{d-1}} &= i \frac{1}{a^d} \sum_{h=0}^{\infty} c_h \int_{-\infty}^{\infty} d\omega \omega \frac{d}{d\omega} \log \left(\omega a J_{h-1+\frac{d}{2}}(|\omega|a) H_{h-1+\frac{d}{2}}^{(1)}(|\omega|a) \right) \\ \frac{F_{S_{d-1},[26]}^{\text{div}}}{A_{d-1}} &= i \frac{1-d}{a^d} \sum_{h=0}^{\infty} c_h \int_{-\infty}^{\infty} d\omega. \end{aligned} \quad (5.2)$$

and the coefficients are given by

$$c_h = \frac{(h-1+\frac{d}{2})\Gamma(h+d-2)}{2^d \pi^{\frac{d+1}{2}} h! \Gamma(\frac{d-1}{2})}. \quad (5.3)$$

A_{d-1} is the area of the $d-1$ -sphere with radius a . All the terms are real upon rotation to Euclidean time, here for convenience we keep the Lorentzian integrals. The result Eq. (5.1) is obtained based on the difference between the radial component of the stress tensor on each side of the sphere. In our language, this is equivalently obtained by considering the sphere as a rigid source with infinite density and deforming it along the radial flow $\mathbf{L} = \mathbf{e}_r$.

The F_S^{fin} term is finite for any d different from positive even integers. The divergence showing up when $d = 2k$, $k = 1, 2, \dots$ is a familiar feature in QFT that can be treated in the framework of renormalization. This physical divergence is not our focus here. In contrast, the F_S^{div} is infinite for any $d \neq 1$. This behavior is not the one of a meromorphic function in d , and should thus draw our attention.

In [26] it was nicely observed that for $d < 1$ the $\sum_{h=0}^{\infty} c_h$ series vanishes identically. A proposal was then made to remove the F^{div} term using an analytical continuation of d to the $d < 1$ region. In summary the argument amounts to stating that since in this region one has $\sum_{h=0}^{\infty} c_h = 0$ identically, any term constant in h arising from the integral is irrelevant since it is multiplied by zero and can thus be subtracted. Notice that the proposed argument is different from usual dimensional regularization which simply turns the quantity of interest into a meromorphic function of d .

An issue remains, however, as $\sum_{h=0}^{\infty} c_h = 0$ in the $d < 1$ region only guarantees that the divergent term F^{div} takes the indefinite form “ $0 \times \infty$ ”. As a result, even if one requires the $\sum_{h=0}^{\infty} c_h$ sum to vanish for any $d > 1$ by analytical continuation of zero, the proposed method remains inconclusive in the sense that $0 \times \infty$ is undefined. For this reason, we will see that the use of our formalism (namely the quantum work on a Dirichlet shell Eq. (3.18) together with matter conservation) allows one to bypass these ambiguities and make the result finite.

5.3 The Quantum Work on the Dirichlet Sphere

We now proceed with our calculation of the quantum work on the Dirichlet sphere with radial deformation. We first define the source and the deformation. We consider a source with the geometry of a spherical shell of width η and with a finite number density n in the $\eta \rightarrow 0$ limit,

$$J_{\eta}(\mathbf{x}) = \frac{n\lambda}{\eta} \mathbf{1}_{a-\frac{\eta}{2} < r < a+\frac{\eta}{2}}(\mathbf{x}) \quad (5.4)$$

The propagator in the presence of this source is denoted by $\Delta_S(x, x')$. The boundary of the shell for small η is identified with $\partial S_{\eta \rightarrow 0} = S_{\text{in}} \cup S_{\text{out}}$ where $S_{\text{in, out}}$ are the $d-1$ -spheres with respective radii $r = a_-, a_+$. The deformation of the source is parametrized by λ and changes the sphere radius such that $a_{\lambda+d\lambda} = a_{\lambda} + Ld\lambda$. Equivalently, in terms of the support function, the deformation is $l_{\lambda+d\lambda}(r) = l_{\lambda}(r - Ld\lambda)$. The deformation flow vector is thus $\mathbf{L} = L\mathbf{e}_r$. Using the conservation equation Eq. (2.9) we can easily derive the variation of density corresponding to such a deformation. We find

$$\partial_{\lambda} n = -\frac{d-1}{a} nL. \quad (5.5)$$

We can now compute the quantum work. Since we are interested in a sphere we can readily use the general formula for the quantum work on a thin shell Eq. (3.18). In the Dirichlet limit the quantum work reads

$$\begin{aligned} W_{S_{d-1}} = & \\ & -\frac{1}{2} A_{d-1} L \left[\partial_{r'} \partial_{r''} \Delta_S(r', t; r'', t) \Big|_{r'=r'' \in S_{\text{out}}} - \partial_{r'} \partial_{r''} \Delta_S(r', t; r'', t) \Big|_{r'=r'' \in S_{\text{in}}} \right] \\ & -\frac{1}{2\Lambda} \int_S d^d \mathbf{x} \Delta_S(x, x) \partial_{\lambda} n_{\lambda} \Big|_{n \rightarrow \infty}. \end{aligned} \quad (5.6)$$

The first term in Eq. (5.6) matches precisely the quantity computed in [26]. Namely we find

$$W_{S_{d-1}} = L \left(F_{S_{d-1}, [26]}^{\text{fin}} + F_{S_{d-1}, [26]}^{\text{div}} \right) - \frac{1}{2\Lambda} \int_S d\sigma(\mathbf{x}) \Delta_S(x, x) \partial_{\lambda} n_{\lambda} \Big|_{n \rightarrow \infty} \quad (5.7)$$

where the components of the force are defined in Eqs. (5.2).

The remaining task is to evaluate the last term in Eq. (5.7), which encodes the variation of density. To this end we first have to evaluate the propagator in the presence of the sphere with finite density. This is done by recomputing the propagator in [26], replacing the two Dirichlet boundary conditions on S by two boundary conditions obtained from integrating

the EOM on the shell enclosing $r = a$ and using the divergence theorem. Introducing the Fourier transform in time $\Delta(x, x) = \int \frac{d\omega}{2\pi} \Delta_\omega(\mathbf{x}, \mathbf{x})$, we find for the propagator at coinciding points

$$\Delta_\omega(a, a) \stackrel{\text{large } n}{\sim} i \frac{\Lambda}{na^{d-1}} \sum_{h=0}^{\infty} \frac{(h-1 + \frac{d}{2})\Gamma(h+d-2)}{2^{d-2}\pi^{\frac{d-1}{2}}h!\Gamma(\frac{d-1}{2})} = i \frac{\Lambda}{na^{d-1}} \sum_{h=0}^{\infty} 4\pi c_h \quad (5.8)$$

with c_h defined in Eq. (5.3). Using the variation of density dictated by matter conservation Eq. (5.5) we then obtain

$$\frac{1}{2\Lambda} \int_S d\sigma(\mathbf{x}) \Delta_S(x, x) \partial_\lambda n_\lambda \Big|_{n \rightarrow \infty} = i \frac{1-d}{a^d} L \sum_{h=0}^{\infty} c_h \int_{-\infty}^{\infty} d\omega = LF_{S_{d-1}, [26]}^{\text{div}}. \quad (5.9)$$

We see that this contribution from the variation of density exactly cancels the divergent piece in Eq. (5.7). It follows that our final result for the quantum work on the Dirichlet sphere amounts to the finite part of the result from [26], namely

$$W_{S_{d-1}} = LF_{S_{d-1}, [26]}^{\text{fin}}. \quad (5.10)$$

The fact that the term from the variation of density cancels the $F_{S_{d-1}, [26]}^{\text{div}}$ divergence upon requirement of matter conservation is non trivial. This cancellation provides a check of our expression for the quantum work on a thin shell Eq. (3.18) and illustrates how the finiteness of the quantum work can manifest itself concretely.

6 Planar Geometry

In this section we evaluate the quantum force in simple planar geometries. While the geometric setup in itself is very well-known, the exact results for the specific quantum force considered here in the case of a massive scalar have not been presented elsewhere. This detailed calculation serves to illustrate how the quantum work remains finite as a result of matter conservation. It also exhibits the transition between the scalar Casimir and Casimir-Polder regimes. The plate-point result obtained here is also key for the search for new particles via atom interferometry that is presented in section 7.

6.1 Force Between two Plates

We focus on the classic Casimir setup with two plates facing each other and separated by a distance ℓ along the z axis. The deformation we consider amounts to a variation of ℓ . We compute the force induced by a massive scalar field with bilinear coupling to the constituents of the plates.

The quantum field Φ is described by the Lagrangian

$$\mathcal{L} = \frac{1}{2}(\partial_\mu \Phi)^2 - \frac{m^2}{2}\Phi^2 - \frac{1}{2\Lambda^2}\Phi^2 J(\mathbf{x}). \quad (6.1)$$

In this application, it is convenient to define J to be the mass density distribution of the sources. In this setting there are five regions along z , with the plates supported on region 1 and 3. The source J is defined as

$$J(z) = \rho_1 \Theta(-\bar{z}_\infty < z < 0) + \rho_3 \Theta(\ell < z < z_\infty) \quad (6.2)$$

The width of the plates is taken to be much larger than the separation, $z_\infty, \bar{z}_\infty \gg \ell$. The fact that the plates actually end instead of continuing to infinity *i.e.* $|z_\infty|, |\bar{z}_\infty| < \infty$ is crucial in order to ensure matter conservation, and therefore that the quantum work is finite as dictated by Eq. (2.23). The effective mass can be written as

$$m^2(z) = m_\infty^2 \Theta(z < -\bar{z}_\infty) + m_1^2 \Theta(-\bar{z}_\infty < z < 0) + m_2^2 \Theta(0 < z < \ell) \\ + m_3^2 \Theta(\ell < z < z_\infty) + m_\infty^2 \Theta(z > z_\infty), \quad (6.3)$$

where

$$m_{\infty,2}^2 = m^2 \quad (6.4)$$

and

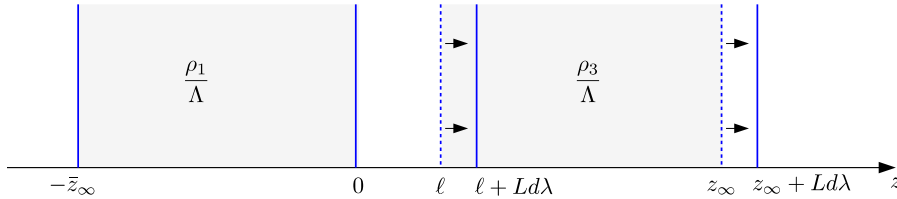
$$m_{1,3}^2 = \frac{\rho_{1,3}}{\Lambda^2} + m^2. \quad (6.5)$$

In Eq. (6.1) the boundary operator amounts to

$$\mathcal{B}_m(\Phi) = \frac{\Phi^2}{2\Lambda^2}. \quad (6.6)$$

Derivative operators such as $\mathcal{B}(\Phi) = \frac{(\partial\Phi)^2}{2\Lambda^4}$ could be treated along the same lines.

The deformation of the source that we consider amounts to shifting the right plate (*i.e.* region 3, the second term in Eq. (6.2)). This corresponds to an infinitesimal shift of ℓ and z_∞ , $\ell_{\lambda+d\lambda} = \ell_\lambda + Ld\lambda$, $z_{\infty,\lambda+d\lambda} = z_{\infty,\lambda} + Ld\lambda$. Notice that the left plate is left untouched, hence \bar{z}_∞ does not vary. Equivalently, in terms of the support function of the right plate, this is described by $l_{\lambda+d\lambda}(z) = l_\lambda(z - Ld\lambda)$. The geometry is summarized as



Since the source moves rigidly, the formula for the quantum work Eq. (4.1) applies and a quantum force can be defined out from the quantum work, $W^{1\text{-loop}} = LF_{\text{quant}}$. In the following we determine F_{quant} .

Propagator

The Feynman propagator in position-momentum space, defined by

$$\Delta(x, x') = \int \frac{d^3p}{(2\pi)^3} e^{ip^\alpha(x-x')_\alpha} \Delta_p(z, z') \quad (6.7)$$

with (p^α, z) , $\alpha = (0, 1, 2)$, has been calculated in the presence of a piece-wise constant mass in [23]. Defining the z -dependent momentum with the Feynman ϵ -prescription

$$\omega(z) = \sqrt{(p_0)^2 - (p_1)^2 - (p_2)^2 + i\epsilon - m^2(z)}, \quad (6.8)$$

the homogeneous equation of motion becomes

$$(\partial_z^2 + \omega^2(z))\Phi(z) = 0 \quad (6.9)$$

whose solutions in a given region i are simply $e^{\pm i\omega_i z}$. The solution everywhere can be found by continuity of the solution and its derivative at each of the interfaces. The propagator is obtained by solving the equations of motion in the five regions and matching them at the boundary. Details can be found in the appendix of [23]. For the calculation of the quantum force, we will only need to evaluate the propagator at coinciding points on the two boundaries of the right-hand plate, $z = \ell$ and $z = z_\infty$.

Quantum Force

The deformation of the source term is found to be

$$\partial_\lambda J = -(\rho_3 - \rho_2)L (\delta(z - \ell) - \delta(z - z_\infty)) . \quad (6.10)$$

Putting this variation back into the definition of the quantum work, we can factor out the L term and obtain the quantum force as defined in Eq. (4.1). As a result the quantum force is given by

$$\begin{aligned} F_{\text{quant}} &= \frac{1}{2}(m_3^2 - m_2^2) \int d^2 \mathbf{x}_\parallel (\Delta(x^\alpha, \ell; x^\alpha, \ell) - \Delta(x^\alpha, z_\infty; x^\alpha, z_\infty)) \\ &= \frac{1}{2}(m_3^2 - m_2^2) \int d^2 \mathbf{x}_\parallel \int \frac{d^3 p}{(2\pi)^3} (\Delta_p(\ell, \ell) - \Delta_p(z_\infty, z_\infty)) \end{aligned} \quad (6.11)$$

with $\mathbf{x}_\parallel = (x_1, x_2)$. The cancellation between the divergent parts of the two propagators at coinciding points is evident in Eq.(6.11), using the fact that the divergence is location-independent. In the second line we have introduced the propagator in position-momentum space. Here we have explicitly

$$\Delta_p(\ell, \ell) - \Delta_p(z_\infty, z_\infty) = \frac{(\omega_1 + \omega_2) + e^{2i\ell\omega_2}(\omega_2 - \omega_1)}{(\omega_1 + \omega_2)(\omega_2 + \omega_3) - e^{2i\ell\omega_2}(\omega_2 - \omega_1)(\omega_2 - \omega_3)} - \frac{1}{\omega_2 + \omega_3} . \quad (6.12)$$

with $\omega_i = \sqrt{(p_\alpha)^2 + i\epsilon - m_i^2}$.

The surface integral $\int d^2 \mathbf{x}_\parallel = S$ is factored out hence defining a pressure. The final expression for the quantum pressure between the two plates (*i.e.* regions 1 and 3) is then

$$\frac{F_{\text{quant}}}{S} = \int_0^\infty \frac{dk k^2}{2\pi^2} \frac{\gamma_2(\gamma_2 - \gamma_1)(\gamma_2 - \gamma_3)}{(\gamma_2 - \gamma_1)(\gamma_2 - \gamma_3) - e^{2\ell\gamma_2}(\gamma_1 + \gamma_2)(\gamma_2 + \gamma_3)} \quad (6.13)$$

after Wick's rotation with $\omega_i = i\gamma_i = i\sqrt{k^2 + m_i^2}$. This is the general expression of the plate-plate quantum pressure in the presence of a scalar coupled quadratically to matter.

In the limit of large density-induced effective mass $m_{1,3} \rightarrow \infty$, the general expression Eq. (6.13) becomes

$$\frac{F_{\text{quant}}}{S} = \int_0^\infty \frac{dk k^2}{2\pi^2} \frac{\gamma_2}{1 - e^{2\ell\gamma_2}}. \quad (6.14)$$

In this limit the effective mass in the plates become so large that the field obeys Dirichlet boundary conditions. Accordingly, Eq. (6.14) matches exactly the Casimir pressure from a massive scalar with Dirichlet boundary conditions. For a massless scalar the integral can be explicitly performed and we retrieve

$$\frac{F_{\text{quant}}}{S} = -\frac{\pi^2}{480\ell^4}. \quad (6.15)$$

This is the classic Casimir pressure for a massless scalar field.

In the limit of small density-induced effective mass defined as $(m_{1,3}^2 - m_2^2)/m_2^2 \ll 1$, *i.e.* when the contribution of the density to the effective mass is small with respect to the fundamental mass, the pressure becomes

$$\frac{F_{\text{quant}}}{S} = -(m_1^2 - m_2^2)(m_3^2 - m_2^2) \int_0^\infty \frac{dk k^2}{2\pi^2} \frac{e^{-2\ell\gamma_2}}{16(\gamma_2)^3}. \quad (6.16)$$

We checked that this corresponds exactly to the Casimir-Polder force integrated over regions 1 and 3. We will see how this calculation can be cross-checked in the next example.

In summary, we have verified that both the scalar Casimir and scalar Casimir-Polder pressures are recovered as limits of the more general expression of the plate-plate quantum pressure Eq. (6.13). Qualitative considerations are given in the next example.

On Finiteness

In Eq. (6.11) we have observed the cancellation between the divergent piece of $\Delta_p(\ell, \ell)$ and $\Delta_p(z_\infty, z_\infty)$ in the integrand. This cancellation makes the expression for the force finite. To illustrate how the presence of the $\Delta_p(z_\infty, z_\infty)$ term is tied to matter conservation, we consider the following counterexample.

Let us imagine that we ignored the displacement of the outer edge ($z = z_\infty$) of the plate. This would imply that the matter of the plate is not conserved since the plate's width would change while the density remains constant. In such a setup, the result would be the same as Eq. (6.11) but without the $\Delta_p(z_\infty, z_\infty)$ contribution. Therefore the expression would be infinite. This simple counterexample illustrates that, when dropping the requirement of matter conservation, the prediction of the force becomes infinite *i.e.* property (2.23) does not hold.

6.2 Force Between a Plate and a Point Source

As a third application of our formalism, we focus on the interaction between a point particle and a plate. As before we assume the Lagrangian

$$\mathcal{L} = \frac{1}{2}(\partial_\mu\Phi)^2 - \frac{m^2}{2}\Phi^2 - \frac{1}{2\Lambda^2}\Phi^2 J(\mathbf{x}). \quad (6.17)$$

The plate is supported on $z < 0$ and has mass density ρ_1 . The source is taken to be

$$J(\mathbf{x}) = \rho_1 \Theta(-z_\infty < z < 0) + m_N \delta^2(\mathbf{x}_\parallel) \delta(z - \ell). \quad (6.18)$$

The mass of the point particle is m_N . We define the effective mass of Φ in the plate as

$$m_1^2 = \frac{\rho_1}{\Lambda^2} + m^2 \quad (6.19)$$

which depends on the coupling to matter, $\frac{1}{\Lambda^2}$. The effective mass of Φ is then piecewise constant,

$$m^2(z) = m_\infty^2 \Theta(z < -z_\infty) + m_1^2 \Theta(-z_\infty < z < 0) + m_2^2 \Theta(z > 0) \quad (6.20)$$

with $m_{\infty,2} = m$.

The deformation we consider is an infinitesimal shift of the point particle position ℓ , $\ell_{\lambda+d\lambda} = \ell_\lambda + Ld\lambda$. The geometry is summarized as



Propagator

The Feynman propagator in position-momentum space (p^α, z) , $\alpha = (0, 1, 2)$ in the presence of a piecewise constant mass has been calculated in [23]. The effect of the point source on the propagation is negligible.¹⁴ For the present calculation, if the frame is chosen such that the deformation changes the position of the point source and not of the plate, one can safely ignore the region at $-z_\infty$ and thus consider the propagator over two regions, with $m^2(z) = m_1^2 \Theta(z < z_{12}) + m_2^2 \Theta(z > z_{12})$. The propagator is found to be

$$\Delta_p(z, z') = \begin{cases} \frac{e^{i\omega_2(z > -z <)} E_2(z <)}{2\omega_2} & z_{12} < z < \\ \frac{e^{i(\omega_2(z > -z_{12}) - \omega_1(z < -z_{12}))}}{\omega_1 + \omega_2} & z < < z_{12} < z > \\ \frac{e^{i\omega_1(z > -z <)} E_1(z >)}{2\omega_1} & z > < z_{12} \end{cases} \quad (6.21)$$

where

$$\begin{aligned} E_1(z) &= 1 + e^{i2(z_{12}-z)\omega_1} \frac{\omega_1 - \omega_2}{\omega_1 + \omega_2} \\ E_2(z) &= 1 + e^{i2(z-z_{12})\omega_2} \frac{\omega_2 - \omega_1}{\omega_1 + \omega_2}. \end{aligned} \quad (6.22)$$

¹⁴This can be checked by evaluating the dressed propagator in energy-position space (p_0, \mathbf{x}) . In the resummed propagator, the effect of the insertion is small within the EFT validity range, leaving the term with one point source insertion as the main non-vanishing contribution to the quantum work.

We have defined $z_{<} = \min(z, z')$ and $z_{>} = \max(z, z')$. We have introduced $\omega_i = \sqrt{(p_\alpha)^2 - m_i^2 + i\epsilon}$. The ϵ prescription guarantees that the propagators decay at infinity. The E_1, E_2 functions essentially describe how the presence of the boundary affects the propagator with both endpoints in the same region. When the boundary z_{12} is rejected to infinity, one recovers the usual expression for a fully homogeneous space.

Quantum Force

The deformation of the source is

$$\partial_\lambda J = -m_N L \delta^2(\mathbf{x}_\parallel) \partial_z \delta(z - \ell). \quad (6.23)$$

Using this expression into the quantum work, one obtains after one integration by parts the quantum force

$$\begin{aligned} F_{\text{quant}} &= -\frac{1}{2} \frac{m_N}{\Lambda^2} \partial_z \Delta_J(x^\alpha, z; x^\alpha, z)|_{z \rightarrow \ell} \\ &= -\frac{1}{2} \frac{m_N}{\Lambda^2} \int \frac{d^3 p}{(2\pi)^3} \partial_z \Delta_J(\mathbf{k}; z, z)|_{z \rightarrow \ell} \end{aligned} \quad (6.24)$$

In the last line we have introduced the position-momentum space propagator.

Using Eq. (6.21) with $z_{12} = 0$ since the plate is placed at the origin, we have

$$\begin{aligned} F_{\text{quant}} &= -\frac{m_N}{\Lambda^2} \frac{1}{2} \int \frac{d^3 p}{(2\pi)^3} \frac{1}{2\omega_2} \partial_z E_2(z)|_{z=\ell} \\ &= -(m_1^2 - m_2^2) \frac{m_N}{\Lambda^2} \frac{1}{4\pi^2} \int dk k^2 \frac{e^{-2\ell\gamma_2}}{(\gamma_1 + \gamma_2)^2} \end{aligned} \quad (6.25)$$

where we have performed a Wick rotation and introduced $\gamma_i = \sqrt{k^2 + m_i^2}$. This is the general expression of the plate-point quantum force in the presence of a scalar coupled quadratically to matter. Diagrammatically, the particle will interact with the plate via loops starting at the point particle, going into the plate and coming back to the point particle.

In the limit of large density-induced effective mass $m_1 \rightarrow \infty$, the force takes the form

$$F_{\text{quant}} = -\frac{m_N}{\Lambda^2} \frac{1}{4\pi^2} \int dk k^2 e^{-2\ell\gamma_2}. \quad (6.26)$$

This is the limit for which the density is so large that the field is repelled by the plate and the field obeys Dirichlet boundary conditions at the boundary of the plate. We refer to this case as the Casimir limit. In the massless case we obtain

$$F_{\text{quant}} = -\frac{m_N}{16\pi^2 \Lambda^2} \frac{1}{\ell^3}. \quad (6.27)$$

In the limit of small density-induced effective mass we expand in $(m_1^2 - m_2^2) \ll m_i^2$ and obtain

$$F_{\text{quant}} = -(m_1^2 - m_2^2) \frac{m_N}{\Lambda^2} \frac{1}{4\pi^2} \int dk k^2 e^{-2\ell\gamma_2} \frac{1}{4\gamma_2^2} \quad (6.28)$$

In the massless case we obtain

$$F_{\text{quant}} = -\frac{m_1^2 m_N}{16\pi^2 \Lambda^2} \frac{1}{\ell}. \quad (6.29)$$

This is the Casimir-Polder limit. As a cross check, in the Appendix we show that this limit is exactly recovered by integrating the point-point Casimir-Polder potential over the extended source.

In summary, we have verified that both the scalar Casimir and scalar Casimir-Polder pressures are recovered as limits of the more general expression of the plate-point quantum pressure Eq. (6.13). The two limits of the massless formula Eqs. (6.27) and (6.29) make transparent that there is a transition between the two regimes as a function of the separation ℓ . Namely, the Casimir regime occurs for $\ell \gg m_1^{-1}$ while the Casimir-Polder regime occurs for $\ell \ll m_1^{-1}$, with $m_1^2 = \frac{\rho_1}{\Lambda^2}$. One way to think about this phenomenon is that, while at large distance the plate behaves as a mirror, leading to a Casimir force, at short distance the quantum fluctuations start penetrating the mirror. As a result the behaviour of the Casimir force gets softened into the the Casimir-Polder one at short distance. This behaviour is confirmed numerically.

7 Bounding Quantum Forces with Atom Interferometry

7.1 The setting

In this section we calculate a somewhat more evolved observable in the context of atom (or neutron) interferometry experiments. Namely we compute the matter-wave phase shift measurable in atom interferometers, which is generated in the presence of a quantum force between the atom and a neighbouring plate. The calculation uses the results from section 6.2.

Atom interferometry has been used to test gravity (see *e.g.* [44–47]) and to search for classical fifth forces, often in the context of dark energy-motivated models [17, 48–50]. Interferometry has never been used to search for quantum forces such as the one modelled by the scalar field used throughout this paper. In this section we thus *i)* compute the phase shift induced by a quantum force and *ii)* demonstrate that interferometry is a competitive method to search for a dark field bilinearly coupled to matter.

Our focus is on a setup which is essentially an adaptation of the simplest “Kasevich-Chu” experiment (see [44–46], and *e.g.* [47] for a review). We describe briefly the setup and refer to the above references and to *e.g.* [51] for further details. Atom or neutron interferometry uses the difference of phase of two coherent wavepackets following two different spacetime paths as shown in Fig. 4. The two paths amount to two broken worldlines, ACB and ADB , with a change of direction at C and D respectively, and with same endpoint B . The changes of velocity of the wavepackets are induced by laser pulses.

We assume that the interferometry experiment is carried out along the z axis over a plate located at $z = 0$. We assume that the setup is oriented horizontally at the surface of the Earth since we are not interested in measuring the strength of the gravity field. The phase shift is caused by the force between the atom and the plate. Experimentally, the

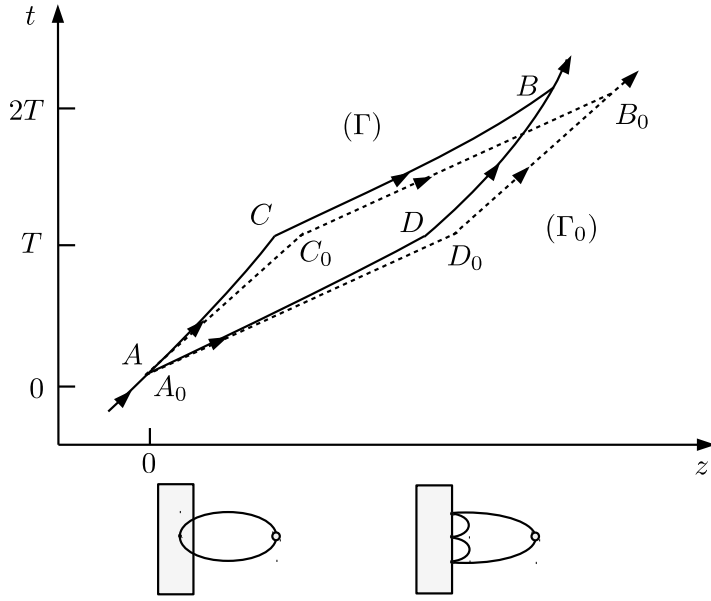


Figure 4. Spacetime paths followed by the atoms in the interferometer. The path in the presence of the force (Γ , plain lines) is deformed with respect to the path in the absence of the force (Γ_0 , dotted lines). The pictures indicate the asymptotic behaviors (Casimir-Polder and Casimir) of the force between the atom and the plate.

plate might be a large ball whose radius is assumed to be much larger than the length of Γ . In this setup the potential $V(z)$ is the one for the plane-point quantum force derived in section 6.2.

Using the WKB approximation, the leading phase shift between the two paths induced by a potential $V(z)$ is given by (see [51])

$$\delta\phi = - \int_{\Gamma_0} dt V(z(t)) \quad (7.1)$$

where $\Gamma_0 = A_0C_0B_0D_0$ denotes the unperturbed closed path and $z(t)$ the corresponding classical trajectory of the wavepackets. Along each segment of Γ_0 , the trajectories are straight,

$$z(t) = z_i + v_i(t - t_i). \quad (7.2)$$

The velocities along each segment of the path can in general differ. In the present setup the time spacing between each pulse is T and the velocities on the segments of Γ_0 are $v_{A_0C_0} = v_{D_0B_0} = v$, $v_{C_0B_0} = v_{A_0D_0} = v'$, as shown in Fig. 4.

7.2 Computing the Phase Shift

We consider the scalar model defined in Eq. (6.2), where the fundamental mass of the field is denoted by m and the mass density of the plate is denoted ρ . The effective mass of the

Φ field for $z < 0$ and $z > 0$ is given by $m_1^2 = \frac{\rho}{\Lambda^2} + m^2$ and $m_2^2 = m^2$. The plane-point force (6.25) derives from a potential $F(\ell) = -\frac{\partial V(\ell)}{\partial \ell}$ given by

$$V(\ell) = -\frac{m_N \rho}{\Lambda^4} \frac{1}{4\pi^2} \int dk k^2 \frac{e^{-2\ell \gamma_2}}{2\gamma_2(\gamma_1 + \gamma_2)^2} \quad (7.3)$$

where ℓ is the distance from the particle to the plate, here taken to be along the z direction. Let us consider one segment of the path Γ_0 where the particle evolves between times t_i and t_j , where i, j denote the endpoints of the segment. The associated phase shift is

$$\delta\phi_{ij} = \int_{t_i}^{t_j} dt \frac{m_N \rho}{\Lambda^4} \frac{1}{4\pi^2} \int dk k^2 \frac{e^{-2(z_i + v(t-t_i)) \gamma_2}}{2\gamma_2(\gamma_1 + \gamma_2)^2} \quad (7.4)$$

$$= \frac{1}{v} \frac{m_N \rho}{\Lambda^4} \frac{1}{4\pi^2} \int dk k^2 \frac{e^{-2z_i \gamma_2} - e^{-2z_j \gamma_2}}{4\gamma_2^2(\gamma_1 + \gamma_2)^2} \quad (7.5)$$

This is an exact result following from the exact expression Eq. (7.3). If one instead used the approximate expressions for either the Casimir or the Casimir-Polder regime to compute the phase shift, one would need to ensure that all distances involved are respectively much bigger or much smaller than the Compton wavelength in the plate, m_1^{-1} (see section 6). Since in the interferometry experiment the separation between the point source and the plane varies, using either the Casimir or the Casimir-Polder approximation may potentially give an erroneous result. The phase shift calculation provides a concrete example of prediction for which the use of the exact result Eq. (7.3) is in general mandatory.

7.3 Limits

The phase shift given by Eq. (7.5) can be further evaluated in some limits when taking $m = 0$. All approximations below have been checked numerically.

7.3.1 $m_1 z_i \gg 1, m_1 z_j \gg 1$

This case amounts to computing the phase shift in the Casimir regime. It is obtained by approximating $\gamma_1 + \gamma_2 \approx m_1$ in the denominator of Eq. (7.5). We obtain

$$\delta\phi_{ij} = \int_{t_i}^{t_j} dt \frac{m_N}{32\pi^2 \Lambda^2 z^2} \quad (7.6)$$

$$= \frac{m_N(z_j - z_i)}{32\pi^2 \Lambda^2 v z_i z_j} = \frac{m_N(t_j - t_i)}{32\pi^2 \Lambda^2 z_i z_j}. \quad (7.7)$$

The overall factor Λ^{-2} is characteristic of the Casimir regime.

7.3.2 $m_1 z_i \ll 1, m_1 z_j \ll 1$

This case would amount to computing the phase shift in the Casimir-Polder regime. However, approximating $\gamma_1 + \gamma_2 \approx 2k$ in the denominator gives a divergent result, therefore we have to go beyond the Casimir-Polder approximation to obtain a finite expression. This is

possible only in our formalism: the small but nonzero effective mass in the plate regularizes the divergence. It is obtained by taking $\gamma_1 + \gamma_2 \approx 2k + \frac{m_1^2}{2k}$ in the denominator. We obtain

$$\delta\phi_{ij} = \frac{m_N(t_j - t_i)\rho}{128\pi^2\Lambda^4} \left(\frac{1}{2} - \gamma + \frac{z_j \log\left(\frac{\Lambda}{z_j\sqrt{\rho}}\right) - z_i \log\left(\frac{\Lambda}{z_i\sqrt{\rho}}\right)}{z_j - z_i} \right) \quad (7.8)$$

The overall Λ^{-4} is characteristic of the Casimir-Polder regime.

7.3.3 $m_1 z_i \ll 1, m_1 z_j \gg 1$

In this nontrivial case we do not find an accurate approximation, only expressions valid up to $O(1)$ uncertainty, which are nevertheless very useful. Taking $\gamma_1 + \gamma_2 \approx m_1$ in the denominator gives

$$\delta\phi_{ij} = \frac{m_N(t_j - t_i)\rho}{16\pi^2 z_j \Lambda^3}. \quad (7.9)$$

Taking $\gamma_1 + \gamma_2 \approx 2k + m_1^2/2k$ in the denominator gives

$$\delta\phi_{ij} = \frac{m_N(t_j - t_i)\rho}{128\pi z_j \Lambda^3}. \quad (7.10)$$

The exact result lies in between these two expressions. We can see that the overall scaling for this case is Λ^{-3} .

7.4 Sensitivity to New Particles

The phase shift over the closed path Γ_0 can be written as $\Delta\Phi = a\kappa T^2$, where $\kappa = M(v - v')$ is the transferred momentum from the laser pulses and T is the period of pulses (*i.e.* $2T$ is the total time between splitting (*A*) and recombination (*B*) of the wavepackets, see Fig. 4). The coefficient a has dimension of an acceleration and can be taken as the figure of merit for the precision of the atom interferometer. The sensitivity of existing experiments can typically reach

$$a_{\text{ex}} \sim 10^{-9}g = 10^{-8} \text{ m}^2\text{s}^{-1} \quad (7.11)$$

(see *e.g.* [46]), that we use as our reference value.

The predicted value of a given by the quantum force in our model is easily obtained in the different regimes discussed above. Comparing it to a_{ex} we obtain an experimental bound on the parameters of the Φ field, *i.e.* an exclusion region in the (m, Λ) plane. For better comparison to other experimental constraints we introduce $\bar{\Lambda} = \frac{\Lambda^2}{m_N}$, which then matches the convention in [52].

The result is shown in Fig. 5. In the regime relevant for the presented sensitivities, the phase shift is dominated by the contributions from the segments near the plate, $\delta\phi \approx \delta\phi_{AC} - \delta\phi_{AD}$. Moreover these contributions are typically in the nontrivial regime of section 7.3.3, which depends only on $z_C \approx z_D \equiv \bar{z}$, which we refer to as the length of the arm of the interferometer. The sensitivity greatly increases when \bar{z} decreases, reflecting the fact that the quantum force quickly increases at short distance. The universal diagonal line correspond to the suppression of the quantum force due to the short Compton wavelength

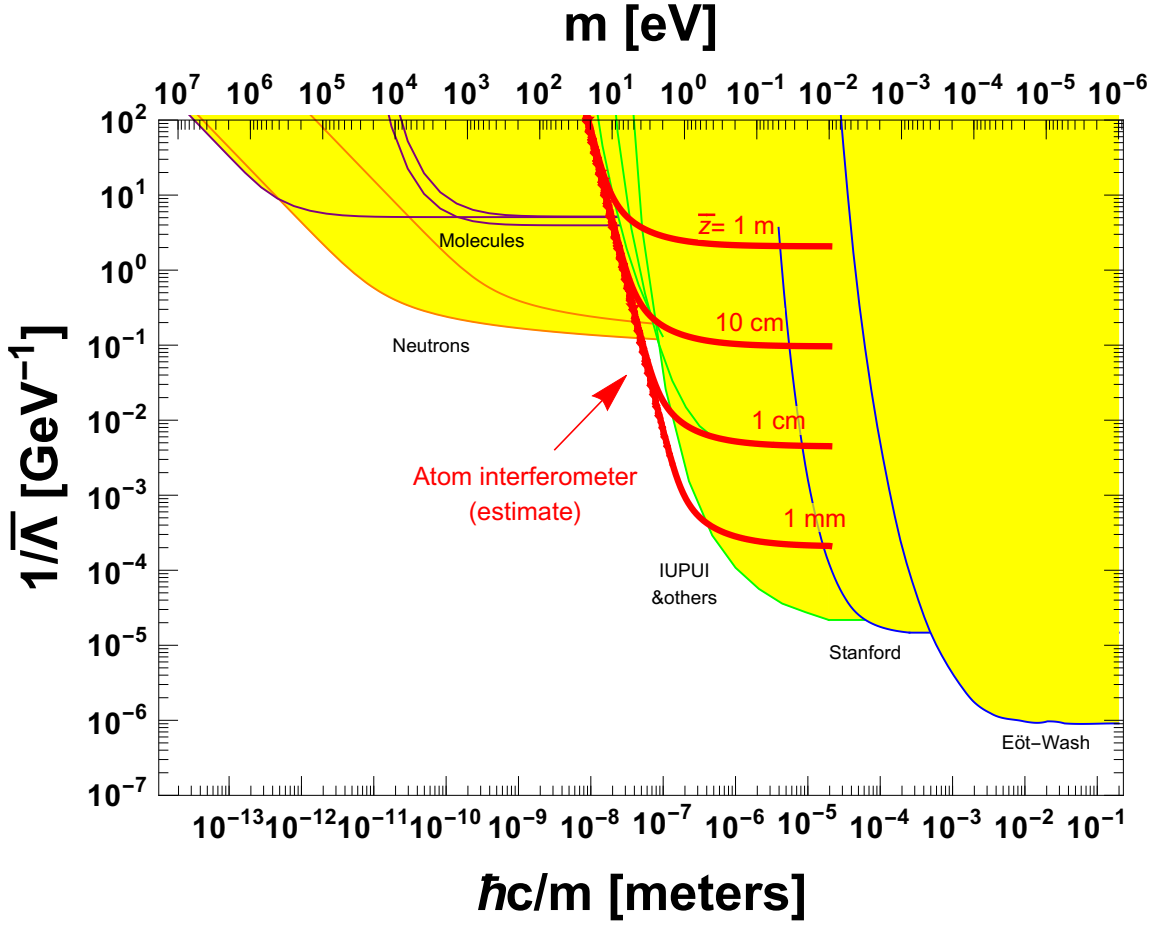


Figure 5. Bounds on the quantum force induced by a scalar field bilinearly coupled to nucleons. Red lines correspond to the sensitivity from atom interferometry using $a_{\text{ex}} = 10^{-8} \text{m}^2 \text{s}^{-1}$. Yellow regions correspond to bounds from other experiments and match Ref. [52]. Those were computed in the Casimir-Polder approximation, except the bound from bouncing neutrons.

of the Φ field. A different sensitivity in a would amount to a change in \bar{z} . All the lines are in the nontrivial regime of section 7.3.3, because for the relevant values of Λ the effective Compton wavelength in the plate m_1^{-1} is much smaller than \bar{z} .

Other experimental bounds are shown in Fig. 5 for comparison.¹⁵ ¹⁶ These other

¹⁵ In the case of dark matter, searches via quantum forces are typically complementary from direct detection searches. The former probe low DM masses while the latter probe high DM masses. Fig. 2 in [31] illustrates this complementarity.

¹⁶ Besides interferometry, another kind of experiment carried out between a particle and a plane is the neutron bouncer, see *e.g.* [53–58]. The quantum levels of the neutrons in the gravitational field of the Earth are probed, via *e.g.* Rabi oscillation techniques, that constrain the difference between energy levels. The quantum levels of the neutrons are classified by an integer n and have the energies $E_n = m_N g z_0 \epsilon_n$ where m_N is the neutron’s mass, g the acceleration of gravity on Earth and $z_0 = (2m_N^2 g)^{-1/3}$ is a characteristic scale of the order of $6 \mu\text{m}$. The number $-\epsilon_n$ are the zeros of the Airy function Ai where the wave functions are $\psi_n(z) \propto \text{Ai}(\frac{z}{z_0} - \epsilon_n)$ and z is the distance to the plate. The perturbation to the energy levels due to the anomalous plate-neutron interaction is given by $\delta E_n = \langle \psi_n | V(z) | \psi_n \rangle$ which is constrained by $|\delta E_n -$

bounds have been so far computed only in the Casimir-Polder regime. In light of the present work, we can see that, while this is exact for molecular bounds and neutron scattering, the Casimir-Polder regime is in general only an approximation in the presence of macroscopic bodies. Using the exact prediction would tend to weaken the bound (see section 6).

We can thus conclude that atom interferometry turns out to be rather competitive method to search for quantum dark forces, provided the interferometer arms (or at least those near the plate, *i.e.* AC and AD) have length below $\bar{z} \sim 10$ cm. This is a reasonable length scale from the experimental viewpoint, which already appears in recent experiments such as the one of [17].

8 Conclusion

How does a classical body respond to an arbitrary deformation in the quantum vacuum? This question can be tackled by introducing the notion of quantum work W , an observable quantity which goes beyond the quantum force \mathbf{F} and reduces to $W = \mathbf{F} \cdot \mathbf{L}$ in specific cases when the deformation flow \mathbf{L} is simple enough, *e.g.* when rigid bodies are displaced with respect to each other. In this paper we have studied the quantum work induced by a massive scalar field bilinearly coupled to macroscopic bodies made of classical matter. Unlike for abstract sources, the number densities of such bodies must satisfy the local conservation of matter. We have shown that the prediction of the quantum work turns out to be finite — up to physical, renormalizable divergences — upon requesting conservation of matter. This result applies to any shape and geometry, either rigid or deformable. This is shown both for a renormalizable — possibly strongly-coupled — theory, and in a more general effective field theory setup allowing for higher derivative interactions between the scalar and matter.

Our result about finiteness of the quantum work readily explains why the QFT prediction of quantum forces sometimes feature seemingly “unremovable” divergences for certain geometries. A key example is the quantum work felt by a Dirichlet sphere under a radial deformation. The radial deformation flow is not divergence-free and thus the sphere density must vary to ensure matter conservation. Not taking this into account implies that matter of the sphere is not conserved, thus the finiteness property is not ensured, and therefore the expression of the quantum force can have a spurious divergence. We have explicitly verified that taking into account the variation of the density removes the spurious divergence in the case of the Dirichlet sphere.

When specializing to rigid bodies, the quantum work leads to a quantum force that reduces to the scalar Casimir and Casimir-Polder forces as special limits. There is a clear diagrammatic understanding of this interpolation. In the short distance regime, the main contribution comes from the loop with only one coupling to each body, which corresponds to Casimir-Polder. In the long distance regime, loops with arbitrary number of insertions

$|\delta E_1| \leq 10^{-14}$ eV [57]. The subsequent bound obtained using the particle-plane force Eq. (6.25) is shown in Fig. 5. This bound is subdominant with respect to the other bounds — also when using the Casimir-Polder approximation [58].

contribute, but their resummation amounts to having a Dirichlet condition on the boundary of the bodies, which corresponds to the traditional Casimir setup.

We have computed the quantum forces in plate-plate and plate-point geometries. If, for example, the scalar has zero fundamental mass, in the plate-plate geometry the force behaves as $\frac{1}{\ell^4}$ at long distance (Casimir) and as $\frac{1}{\ell^2}$ at short distance (Casimir-Polder). For plate-point geometry the force behaves as $\frac{1}{\ell^3}$ at long distance (Casimir) and as $\frac{1}{\ell}$ at short distance (Casimir-Polder). For nonzero fundamental mass the two limits can still exist, but the Casimir force drops exponentially at separation $\ell \gg \frac{1}{2m}$.

These results have concrete applications for physical setups aimed at searching for light dark particles. Such particles are ubiquitous in dark matter models, dark energy models, and in extensions of the Standard Model. Here we have briefly illustrated an application of the point-plane quantum force for atom interferometers. In this type of experiment, a non-relativistic atom with trajectory in the vicinity of a large sphere or a plane is sensitive to the existence of a new force, which induces a phase shift that can be computed in the WKB approximation. We have computed the atomic phase shift induced by the scalar quantum force, and point out that the full result (as opposed to a simple Casimir or Casimir-Polder approximation) is required to obtain a sensible prediction. Using inputs from existing experiments, we show that atom interferometry is likely to become a competitive method to search for light dark particles bilinearly coupled to matter, provided that the interferometer arms are shorter than ~ 10 cm, as summarized in Fig. 5. This is a reasonable length scale from the experimental viewpoint, which already appears in setups such as the one of [17].

In future work we will further investigate/revisit the constraints and sensitivities of future experiments to macroscopic dark quantum forces with Casimir-like behaviors.

Acknowledgments

SF thanks Daniel Davies for a useful discussion. This work has been supported by the São Paulo Research Foundation (FAPESP) under grants #2011/11973, #2014/21477-2 and #2018/11721-4, by CAPES under grant #88887.194785, and by the University of California, Riverside.

A Derivation of the Plate-Point Casimir-Polder Potential

The Casimir-Polder potential between a particle and a plate can be obtained by direct calculation in the weak coupling regime (*i.e.* the limit of small density in the plate). We start by computing the potential between two point sources. The corresponding source term is

$$\mathcal{L} \supset -\frac{1}{2}\Phi^2 \left(\frac{m_a}{\Lambda^2} \delta^3(\mathbf{x} - \mathbf{x}_a) + \frac{m_N}{\Lambda^2} \delta^3(\mathbf{x} - \mathbf{x}_b) \right). \quad (\text{A.1})$$

We remind that this is the non-relativistic approximation of the 4-point interaction

$$\mathcal{L} \supset -\frac{1}{2}\Phi^2 \left(\frac{m_a}{\Lambda^2} \bar{\psi}_a \psi_a + \frac{m_N}{\Lambda^2} \bar{\psi}_b \psi_b \right) \quad (\text{A.2})$$

between the scalar and two fermion species. The scattering amplitude with two insertions of two particle-anti particles pairs leads to a bubble diagram which reads

$$i\mathcal{M} = -\frac{m_N m_a}{\Lambda^4} 4m_N m_a \frac{1}{2} \int \frac{d^3 k}{(2\pi)^3} \frac{e^{i\omega_2|z_1-z_2|}}{2\omega_2} \frac{e^{i\omega'_2|z_1-z_2|}}{2\omega'_2} \quad (\text{A.3})$$

where $\omega_2 = \sqrt{k^2 - m_2^2}$, $\omega'_2 = \sqrt{(k+p)^2 - m_2^2}$. The factor of $\frac{1}{2}$ is a symmetry factor and the external fermions are such that their nonrelativistic wavefunctions are normalised as $\bar{u}_a u_a = 2m_a$, $\bar{u}_b u_b = 2m_N$. The non-relativistic scattering potential is given by

$$\begin{aligned} \tilde{V}(p, z_1 - z_2) &= -\frac{\mathcal{M}}{4m_a m_N} \\ &= -i \frac{m_N m_a}{\Lambda^4} \frac{1}{2} \int \frac{d^3 k}{(2\pi)^3} \frac{e^{i\omega_2|z_1-z_2|}}{2\omega_2} \frac{e^{i\omega'_2|z_1-z_2|}}{2\omega'_2}. \end{aligned} \quad (\text{A.4})$$

The spatial potential is then obtained from the Fourier transform of \tilde{V} ,

$$V\left(\sqrt{(z_1 - z_2)^2 + \mathbf{x}_\parallel^2}\right) = \int \frac{d^2 \mathbf{p}_\parallel}{(2\pi)^2} \tilde{V}(\mathbf{p}_\parallel, z_1, z_2) e^{i\mathbf{p}_\parallel \cdot \mathbf{x}_\parallel} \quad (\text{A.5})$$

where $\mathbf{x}_\parallel = (x_1, x_2)$.

We now consider an ensemble of N_1 particle of the species a in a volume V_1 with a number density $n_1 = \frac{N_1}{V_1}$. We average the potential over the plate with a separation ℓ to the point particle as

$$V(\ell) = n_1 \int d^2 \mathbf{x}_\parallel \int_{-\infty}^0 dz_1 \int \frac{d^2 \mathbf{p}_\parallel}{(2\pi)^2} \tilde{V}(\mathbf{p}_\parallel, z_1, \ell) e^{i\mathbf{p}_\parallel \cdot \mathbf{x}_\parallel}. \quad (\text{A.6})$$

The transverse integrals simplify and the potential becomes simply

$$V(\ell) = n_1 \int_{-\infty}^0 dz_1 \tilde{V}(0, z_1, \ell) = -n_1 \frac{m_a m_N}{\Lambda^4} \int \frac{d^3 k_E}{(2\pi)^3} \frac{e^{-2\gamma_2 \ell}}{16(\gamma_2)^3} \quad (\text{A.7})$$

after Wick's rotation. Using $m_1^2 - m_2^2 = n_1 m_a / \Lambda^2$, we find

$$V(\ell) = -(m_1^2 - m_2^2) \frac{m_N}{\Lambda^2} \int \frac{d^3 k_E}{(2\pi)^3} \frac{e^{-2\gamma_2 \ell}}{16(\gamma_2)^3}. \quad (\text{A.8})$$

Finally the force is obtained by taking the derivative with respect to ℓ

$$F = -\partial_\ell V = -(m_1^2 - m_2^2) \frac{m_N}{\Lambda^2} \int \frac{d^3 k_E}{(2\pi)^3} \frac{e^{-2\gamma_2 \ell}}{8(\gamma_2)^2}. \quad (\text{A.9})$$

This reproduces Eq. (6.28).

B On Divergences from the Heat Kernel Expansion

In this appendix we review how the heat kernel expansion allows for a proof of the finiteness of the quantum work at one-loop level under the assumptions that (i) the bodies are incompressible and (ii) the fluctuation is repelled from the sources so that we can set boundary conditions at the source surfaces, analogously to the Dirichlet limit described in section 4.4. We will then see that the argument fails when condition (i) is dropped *i.e.* considering a compressible body, which signals the need for an approach that includes matter conservation.

We essentially review the exposition from [10]. We consider two rigid bodies such that $J = J_1 + J_2$ as in section 4. First of all, let us rewrite the scalar action as

$$S(\Phi) = S_2(\Phi) + S_{\text{int}}(\Phi) \quad (\text{B.1})$$

where we have included the J -dependent contribution to the effective mass in the quadratic part of the action. This action reads

$$S_2(\Phi) = -\frac{1}{2} \int d^4x \Phi \square_J \Phi \quad (\text{B.2})$$

where \square_J is the operator which includes the effective mass term. In the renormalizable case, this is simply

$$\square_J = \square + m^2 + \frac{J}{\Lambda}. \quad (\text{B.3})$$

In the EFT case, higher order derivatives are present.

We assume weak coupling. When the sources are static, the quantum vacuum energy reads

$$E(J) = \frac{i}{T} \ln Z(J) = -\frac{i}{2T} \text{Tr} \ln \square_J + \frac{i}{T} W_2(J) \quad (\text{B.4})$$

where the first contribution is the one-loop contribution to the vacuum diagrams, and $W_2(J)$ is the sum over all connected vacuum diagrams at two loops and higher. Here we focus on the one-loop contribution, which is independent of other possible interactions (*e.g.* polynomial self-interactions of Φ). The one-loop piece can be evaluated using the heat kernel $K_J = e^{-t\square_J}$ and its trace as

$$\text{Tr} \ln \Delta_J = -\int_0^\infty \frac{dt}{t} \text{Tr} K_J(t). \quad (\text{B.5})$$

See [59] for a conceptual review on heat kernel methods. The trace of the heat kernel has a $t \rightarrow 0$ expansion

$$\text{Tr} K_J(t) = \frac{1}{(2\pi t)^{3/2}} (a_0 + a_{1/2} t^{1/2} + a_1 t + a_{3/2} t^{3/2} + \dots) \quad (\text{B.6})$$

We can see that the heat kernel coefficients $a_{n/2}$, $n = 0, \dots, 3$ are responsible for the divergences of $E(J)$. These coefficients are universal local quantities [10, 59] and can be expressed as volume integrals over the support of the J_i sources and surface integrals over

their boundaries, ∂J_i . The first coefficient simply amounts to the volume of the support of the fluctuation, which is the space outside of the sources,

$$a_0 = V - V_1 - V_2 \quad (\text{B.7})$$

with $V_{1,2} = \text{Vol}(J_{1,2})$ and V the volume of the total space. Depending on the geometric setup, these various volumes may be finite or infinite, this is a minor detail in the argument.

We can now vary the quantum vacuum energy under some deformation flow. We use the notation of section 2. In the case of a rigid deformation flow (*i.e.* satisfying $\boldsymbol{\partial} \cdot \mathbf{L} = 0$), *e.g.* two bodies moving apart, the coefficients are independent of the relative position of the bodies [10, 60]. As a result all the divergences cancel when computing the quantum work by varying the relative position of the bodies. This is easily illustrated at the level of the a_0 coefficient, for which we simply have

$$\partial_\lambda a_0 = -\partial_\lambda \int_{J_\lambda} d^d \mathbf{x} = - \int_{J_\lambda} d^d \mathbf{x} \boldsymbol{\partial} \cdot \mathbf{L} = 0. \quad (\text{B.8})$$

where we have used that $\partial_\lambda V = 0$. Therefore under the assumption of incompressibility the quantum work is finite. This is a version of the classic argument given in [10].

In contrast, in the case of a deformation flow for which $\boldsymbol{\partial} \cdot \mathbf{L} \neq 0$, *i.e.* dropping the assumption of incompressibility, we can see that $\partial_\lambda a_0 \neq 0$, which then results in a divergence in the quantum work. There is no parameter in the Lagrangian into which this divergence could be absorbed, therefore there is no hope to renormalize this divergence away. The only way out we found is to let the number density of the sources vary in such way that matter conservation in the source is satisfied. As shown in section 2, 3.1 and exemplified in section 5, this is the condition that ensures that all possible divergences in the quantum work vanish.

C The Loop Divergence from Momentum Space

We are interested in the loop integral given in Eq. (3.8),

$$I = \left(\prod_{i=1}^q \int d^d \boldsymbol{\mu}_i J(\boldsymbol{\mu}_i) \int dt_i \right) \prod_{i=0}^q \mathcal{B}'' \Delta_0(\mu_i, \mu_{i+1}) \Big|_{\mu_0=x, \mu_{q+1}=x_\epsilon}. \quad (\text{C.1})$$

We introduce the $(d+1)$ -dimensional Fourier transform of the propagators defined as

$$\Delta_0(\mu_i, \mu_{i+1}) = \int \not{d}^{d+1} k e^{ik \cdot (\mu_{i+1} - \mu_i)} \tilde{\Delta}_0(k). \quad (\text{C.2})$$

We introduce the d -dimensional Fourier transform of the sources,

$$J(\boldsymbol{\mu}_i) = \int \not{d}^d \mathbf{k} e^{i\mathbf{k} \cdot \boldsymbol{\mu}_i} \tilde{J}(\mathbf{k}). \quad (\text{C.3})$$

We have defined $\not{d}k = \frac{dk}{2\pi}$. The contraction between the $(d+1)$ -vectors is done using the Minkowski metric $k \cdot y = \eta_{\mu\nu} k^\mu y^\nu$ with $k^\mu = (\omega, \mathbf{k})$. The loop integral becomes

$$I = \int \not{d}^{d+1} k_0 \left(\prod_{i=1}^q \int \not{d}^d \mathbf{p}_i \tilde{J}(\mathbf{p}_i) \right) \left(\prod_{i=0}^q \tilde{B}''(k_{i-1}, k_i) \tilde{\Delta}_0(k_i) \right) e^{ik_q \cdot x_\epsilon - ik_0 \cdot x} \quad (\text{C.4})$$

with $\mathbf{p}_i = \mathbf{k}_i - \mathbf{k}_{i-1}$ the momentum transferred to the source.

Performing the time and position integrals we obtain an integral over the $(d + 1)$ -momentum k_0 running through the loop. The derivative operators in real space become simply multiplying operators depending on the two momenta entering each vertex $\tilde{B}''(k_{i-1}, k_i)$. In the EFT case it contains at least two powers of the momenta.

Since the source J has compact support, the Riemann-Lebesgue lemma guarantees that $\tilde{J}(\mathbf{p})$ vanishes for large momenta and in fact falls off for $|\mathbf{p}| \gtrsim R_J^{-1}$. This implies a smooth cutoff on the value of \mathbf{p} . On the other hand the divergence in I occurs for arbitrarily large loop momentum k_0 . Since the \mathbf{p} are bounded, at large loop momentum we have $k_0 \simeq k_1 \simeq \dots \simeq k_q$, thus the divergent part of the diagram is \mathbf{p} -independent and is only a function of $(x_\epsilon - x) = \epsilon$. Writing $c_J = \int d^d \mathbf{p}_i \tilde{J}(\mathbf{p}_i)$, we have the structure

$$I \approx c_J^q L_\epsilon^{\text{div}} \quad (\text{C.5})$$

where L_ϵ^{div} is the position-independent divergent quantity.

References

- [1] H. B. G. Casimir and D. Polder, *The influence of retardation on the london-van der waals forces*, *Phys. Rev.* **73** (Feb, 1948) 360–372.
- [2] H. B. G. Casimir, *On the Attraction Between Two Perfectly Conducting Plates*, *Indag. Math.* **10** (1948) 261–263.
- [3] K. A. Milton, *The Casimir effect: Recent controversies and progress*, *J. Phys. A* **37** (2004) R209, [[hep-th/0406024](#)].
- [4] G. L. Klimchitskaya, U. Mohideen, and V. M. Mostepanenko, *The Casimir force between real materials: Experiment and theory*, *Rev. Mod. Phys.* **81** (2009) 1827–1885, [[arXiv:0902.4022](#)].
- [5] A. W. Rodriguez, P.-C. Hui, D. P. Woolf, S. G. Johnson, M. Lončar, and F. Capasso, *Classical and fluctuation-induced electromagnetic interactions in micron-scale systems: designer bonding, antibonding, and Casimir forces*, *Annalen der Physik* **527** (Jan., 2015) 45–80, [[arXiv:1409.7348](#)].
- [6] L. M. Woods, D. A. R. Dalvit, A. Tkatchenko, P. Rodriguez-Lopez, A. W. Rodriguez, and R. Podgornik, *Materials perspective on Casimir and van der Waals interactions*, *Rev. Mod. Phys.* **88** (2016), no. 4 045003, [[arXiv:1509.03338](#)].
- [7] G. Bimonte, T. Emig, M. Kardar, and M. Krüger, *Nonequilibrium Fluctuational Quantum Electrodynamics: Heat Radiation, Heat Transfer, and Force*, *Ann. Rev. Condensed Matter Phys.* **8** (2017) 119–143, [[arXiv:1606.03740](#)].
- [8] G. Bimonte and T. Emig, *Unifying Theory for Casimir Forces: Bulk and Surface Formulations*, *Universe* **7** (2021), no. 7 225, [[arXiv:2108.07112](#)].
- [9] G. Bimonte, T. Emig, N. Graham, and M. Kardar, *Something Can Come of Nothing: Quantum Fluctuations and the Casimir Force*, [[arXiv:2202.05386](#)].
- [10] M. Bordag, G. L. Klimchitskaya, U. Mohideen, and V. M. Mostepanenko, *Advances in the Casimir effect*, vol. 145. Oxford University Press, 2009.

- [11] K. A. Milton, *Calculating casimir energies in renormalizable quantum field theory*, *Phys. Rev.* **D68** (2003) 065020, [[hep-th/0210081](#)].
- [12] N. Graham, R. L. Jaffe, V. Khemani, M. Quandt, M. Scandurra, and H. Weigel, *Casimir energies in light of quantum field theory*, *Phys. Lett. B* **572** (2003) 196–201, [[hep-th/0207205](#)].
- [13] R. L. Jaffe, *The Casimir effect and the quantum vacuum*, *Phys. Rev. D* **72** (2005) 021301, [[hep-th/0503158](#)].
- [14] S. Mobassem, *Casimir effect for massive scalar field*, *Mod. Phys. Lett. A* **29** (2014), no. 31 1450160, [[arXiv:1403.0501](#)].
- [15] L. Hui, J. P. Ostriker, S. Tremaine, and E. Witten, *Ultralight scalars as cosmological dark matter*, *Phys. Rev. D* **95** (2017), no. 4 043541, [[arXiv:1610.08297](#)].
- [16] A. Joyce, B. Jain, J. Khoury, and M. Trodden, *Beyond the Cosmological Standard Model*, *Phys. Rept.* **568** (2015) 1–98, [[arXiv:1407.0059](#)].
- [17] P. Hamilton, M. Jaffe, P. Haslinger, Q. Simmons, H. Müller, and J. Khoury, *Atom-interferometry constraints on dark energy*, *Science* **349** (2015) 849–851, [[arXiv:1502.03888](#)].
- [18] B. C. Allanach, *Beyond the Standard Model Lectures for the 2016 European School of High-Energy Physics*, in *2016 European School of High-Energy Physics*, pp. 123–152, 2017. [[arXiv:1609.02015](#)].
- [19] P. Brax, S. Casas, H. Desmond, and B. Elder, *Testing Screened Modified Gravity*, *Universe* **8** (2021), no. 1 11, [[arXiv:2201.10817](#)].
- [20] T. Damour and A. M. Polyakov, *The String dilaton and a least coupling principle*, *Nucl. Phys. B* **423** (1994) 532–558, [[hep-th/9401069](#)].
- [21] J. Khoury and A. Weltman, *Chameleon fields: Awaiting surprises for tests of gravity in space*, *Phys. Rev. Lett.* **93** (2004) 171104, [[astro-ph/0309300](#)].
- [22] J. Khoury and A. Weltman, *Chameleon cosmology*, *Phys. Rev. D* **69** (2004) 044026, [[astro-ph/0309411](#)].
- [23] P. Brax and S. Fichet, *Quantum Chameleons*, *Phys. Rev.* **D99** (2019), no. 10 104049, [[arXiv:1809.10166](#)].
- [24] J. S. Schwinger, L. L. DeRaad, Jr., and K. A. Milton, *Casimir Effect in Dielectrics*, *Annals Phys.* **115** (1979) 1–23.
- [25] M. E. Peskin and D. V. Schroeder, *An introduction to quantum field theory*. Westview, Boulder, CO, 1995.
- [26] C. M. Bender and K. A. Milton, *Scalar casimir effect for a d-dimensional sphere*, *Phys. Rev. D* **50** (Nov, 1994) 6547–6555.
- [27] I. E. Dzyaloshinskii, E. M. Lifshitz, and L. P. Pitaevskii, *GENERAL THEORY OF VAN DER WAALS' FORCES*, *Soviet Physics Uspekhi* **4** (feb, 1961) 153–176.
- [28] G. Feinberg and J. Sucher, *Long-Range Forces from Neutrino-Pair Exchange*, *Phys. Rev.* **166** (1968) 1638–1644.
- [29] G. Feinberg and J. Sucher, *Long-range forces from neutrino-pair exchange*, *Phys. Rev.* **166** (Feb, 1968) 1638–1644.

- [30] J. A. Grifols, E. Masso, and R. Toldra, *Majorana neutrinos and long range forces*, *Phys. Lett.* **B389** (1996) 563–565, [[hep-ph/9606377](#)].
- [31] S. Fichet, *Quantum Forces from Dark Matter and Where to Find Them*, *Phys. Rev. Lett.* **120** (2018), no. 13 131801, [[arXiv:1705.10331](#)].
- [32] A. Costantino, S. Fichet, and P. Tanedo, *Exotic Spin-Dependent Forces from a Hidden Sector*, [arXiv:1910.02972](#). To appear in JHEP.
- [33] N. Graham, R. L. Jaffe, V. Khemani, M. Quandt, M. Scandurra, and H. Weigel, *Calculating vacuum energies in renormalizable quantum field theories: A New approach to the Casimir problem*, *Nucl. Phys. B* **645** (2002) 49–84, [[hep-th/0207120](#)].
- [34] N. Graham, R. L. Jaffe, V. Khemani, M. Quandt, O. Schroeder, and H. Weigel, *The Dirichlet Casimir problem*, *Nucl. Phys. B* **677** (2004) 379–404, [[hep-th/0309130](#)].
- [35] S. A. Franchino-Viñas, M. N. Mantiñan, and F. D. Mazzitelli, *Quantum vacuum fluctuations and the principle of virtual work in inhomogeneous backgrounds*, *Phys. Rev. D* **105** (2022), no. 8 085023, [[arXiv:2110.14692](#)].
- [36] A. V. Manohar, *Effective field theories*, *Lect. Notes Phys.* **479** (1997) 311–362, [[hep-ph/9606222](#)].
- [37] A. V. Manohar, *Introduction to Effective Field Theories*, [arXiv:1804.05863](#).
- [38] Y. Li, K. A. Milton, X. Guo, G. Kennedy, and S. A. Fulling, *Casimir forces in inhomogeneous media: renormalization and the principle of virtual work*, *Phys. Rev. D* **99** (2019), no. 12 125004, [[arXiv:1901.09111](#)].
- [39] S. A. Franchino-Viñas and F. D. Mazzitelli, *Effective action for delta potentials: spacetime-dependent inhomogeneities and Casimir self-energy*, *Phys. Rev. D* **103** (2021), no. 6 065006, [[arXiv:2010.11144](#)].
- [40] S. Fichet, *Field Holography in General Background and Boundary Effective Action from AdS to dS*, [arXiv:2112.00746](#).
- [41] M. Bordag and D. V. Vassilevich, *Nonsmooth backgrounds in quantum field theory*, *Phys. Rev. D* **70** (2004) 045003, [[hep-th/0404069](#)].
- [42] M. Bordag, D. Vassilevich, H. Falomir, and E. M. Santangelo, *Multiple reflection expansion and heat kernel coefficients*, *Phys. Rev. D* **64** (2001) 045017, [[hep-th/0103037](#)].
- [43] T. H. Boyer, *Quantum electromagnetic zero point energy of a conducting spherical shell and the Casimir model for a charged particle*, *Phys. Rev.* **174** (1968) 1764–1774.
- [44] M. Kasevich and S. Chu, *Atomic interferometry using stimulated Raman transitions*, *Phys. Rev. Lett.* **67** (1991) 181–184.
- [45] M. Kasevich and S. Chu, *Measurement of the gravitational acceleration of an atom with a light-pulse atom interferometer*, *Applied Physics B: Lasers and Optics* **54** (May, 1992) 321–332.
- [46] A. Peters, K. Y. Chung, and S. Chu, *Measurement of gravitational acceleration by dropping atoms*, *Nature* **400** (Aug., 1999) 849–852.
- [47] A. Miffre, M. Jacquy, M. Büchner, G. Tréneç, and J. Vigué, *Atom interferometry*, [quant-ph/0605055](#).
- [48] C. Burrage, E. J. Copeland, and E. A. Hinds, *Probing Dark Energy with Atom Interferometry*, *JCAP* **1503** (2015), no. 03 042, [[arXiv:1408.1409](#)].

- [49] M. Jaffe, P. Haslinger, V. Xu, P. Hamilton, A. Upadhye, B. Elder, J. Khoury, and H. Müller, *Testing sub-gravitational forces on atoms from a miniature, in-vacuum source mass*, *Nature Phys.* **13** (2017) 938, [[arXiv:1612.05171](#)].
- [50] D. O. Sabulsky, I. Dutta, E. A. Hinds, B. Elder, C. Burrage, and E. J. Copeland, *Experiment to detect dark energy forces using atom interferometry*, *Phys. Rev. Lett.* **123** (2019), no. 6 061102, [[arXiv:1812.08244](#)].
- [51] P. Storey and C. Cohen-Tannoudji, *The Feynman path integral approach to atomic interferometry: A tutorial*, *J. Phys. II* **4** (1994), no. 11 1999–2027.
- [52] P. Brax, S. Fichet, and G. Pignol, *Bounding Quantum Dark Forces*, *Phys. Rev.* **D97** (2018), no. 11 115034, [[arXiv:1710.00850](#)].
- [53] V. V. Nesvizhevsky, G. Pignol, and K. V. Protasov, *Neutron scattering and extra short range interactions*, *Phys. Rev.* **D77** (2008) 034020, [[arXiv:0711.2298](#)].
- [54] P. Brax and G. Pignol, *Strongly Coupled Chameleons and the Neutronic Quantum Bouncer*, *Phys. Rev. Lett.* **107** (2011) 111301, [[arXiv:1105.3420](#)].
- [55] P. Brax, G. Pignol, and D. Roulier, *Probing Strongly Coupled Chameleons with Slow Neutrons*, *Phys. Rev.* **D88** (2013) 083004, [[arXiv:1306.6536](#)].
- [56] T. Jenke et al., *Gravity Resonance Spectroscopy Constrains Dark Energy and Dark Matter Scenarios*, *Phys. Rev. Lett.* **112** (2014) 151105, [[arXiv:1404.4099](#)].
- [57] G. Cronenberg, P. Brax, H. Filter, P. Geltenbort, T. Jenke, G. Pignol, M. Pitschmann, M. Thalhammer, and H. Abele, *Acoustic Rabi oscillations between gravitational quantum states and impact on symmetron dark energy*, *Nature Phys.* **14** (2018), no. 10 1022–1026.
- [58] P. Brax and M. Pitschmann, *Exact solutions to nonlinear symmetron theory: One- and two-mirror systems*, *Phys. Rev.* **D97** (2018), no. 6 064015, [[arXiv:1712.09852](#)].
- [59] D. V. Vassilevich, *Heat kernel expansion: User’s manual*, *Phys. Rept.* **388** (2003) 279–360, [[hep-th/0306138](#)].
- [60] S. A. Fulling, *Systematics of the relationship between vacuum energy calculations and heat kernel coefficients*, *J. Phys. A* **36** (2003) 6857–6873, [[quant-ph/0302117](#)].